Manuscript Click here to access/download;Manuscript;Prophase Cenp-C-PLOS.pdf

A Dynamic population of prophase CENP-C is required for meiotic chromosome segregation

Jessica E. Fellmeth, Janet Jang, Manisha Persaud, Hannah Sturm, Neha Changela, Aashka Parikh, and Kim S. McKim

Waksman Institute and Department of Genetics, Rutgers, the State University of New Jersey, Piscataway, New Jersey, United States of America.

Correspondence: Kim S. McKim (mckim@waksman.rutgers.edu)

Short Title: CENP-C dynamics and function in meiosis

Corresponding author: Kim S. McKim

190 Frelinghuysen Road,

Piscataway, NJ-08854

848-445-1164

mckim@waksman.rutgers.edu

Abstract

The centromere is an epigenetic mark that is a loading site for the kinetochore during meiosis and mitosis. This mark is characterized by the H3 variant CENP-A, known as CID in *Drosophila*. In *Drosophila*, CENP-C is critical for maintaining CID at the centromeres and directly recruits outer kinetochore proteins after nuclear envelope break down. It is not known, however, if these two functions require the same CENP-C molecules. Furthermore, in *Drosophila* and many other metazoan oocytes, centromere maintenance and kinetochore assembly are separated by an extended prophase. Consistent with studies in mammals, CID is relatively stable and does not need to be expressed during prophase to remain at high levels in metaphase I of meiosis. Expression of CID during prophase can even be deleterious, causing ectopic localization to non-centromeric chromatin, abnormal meiosis and sterility. In contrast to CID, maintaining high levels of CENP-C requires expression during prophase. Confirming the importance of this loading, we found CENP-C prophase loading is required for multiple meiotic functions. In early meiotic prophase, CENP-C loading is required for sister centromere cohesion and centromere clustering. In late meiotic prophase, CENP-C loading is required to recruit kinetochore proteins. CENP-C is one of the few proteins identified in which expression during prophase is required for meiotic chromosome segregation. An implication of these results is that the failure to maintain recruitment of CENP-C during the extended prophase in oocytes would result in chromosome segregation errors in oocytes.

Author Summary

Meiosis in oocytes of diverse organisms, including humans and *Drosophila,* is characterized by a long prophase pause and a cell cycle arrest in meiosis I or meiosis II. These pauses could be a challenge for centromeres, whose components are replenished during G1, and then must remain with the chromosomes until the meiotic divisions. We have investigated the stability, prophase dynamics and function of centromere protein CENP-C. We show that CENP-C expression and loading onto centromeres during prophase is required for multiple meiotic functions. In contrast, the expression of other centromere partners CID/CENP-A and CAL1 is not required during meiotic prophase. Furthermore, expression of CID during prophase can be deleterious and result in ectopic kinetochore formation. CENP-C loading in prophase is required for sister centromere cohesion and kinetochore assembly. Our results provide the first description of CENP-C dynamics during meiosis and show that prophase expression is required for oocyte spindle assembly and function. CENP-C is among a small number of proteins that are required for the meiotic divisions but are loaded prior to prometaphase. Failure to maintain these proteins during the long prophase of oocyte meiosis may contribute to the increased aneuploidy associated with advanced maternal age.

58 ## Introduction

59 The chromatin of the centromere is characterized by an H3 variant known as CENP-A
60 rather than a specific sequence [1, 2]. One of its functions is to recruit kinetochore proteins for
61 meiosis and mitosis [3]. Failure to maintain the centromere after DNA replication or failure to
62 recruit an effective kinetochore during M-phase can result in chromosome segregation defects. In
63 *Drosophila*, CENP-A is encoded by the *cid* gene [4]. CENP-A interacts with the "constitutive
64 centromere associated network" (CCAN) complex in a wide variety of organisms such as
65 humans and yeast [3]. The CCAN contains many proteins that form multiple links between the
66 inner centromere and the outer kinetochore. In many vertebrate cells, two pathways defined by
67 the components CENP-T and CENP-C provide the link between the centromere and outer
68 kinetochore [5]. In some cases, one of these pathways has been lost during evolution. *C. elegans*
69 and *Drosophila* are examples where most or all CCAN proteins have been lost and CENP-C
70 forms the only linkage between the inner centromere and outer kinetochore.

71 Centromeres are maintained by loading new CENP-A once per cell cycle, but unlike
72 replication-dependent histones, this does not occur during S-phase. Thus, CENP-A levels are
73 reduced during S-phase and return to normal levels once during the cell cycle. The timing of
74 CENP-A loading varies in different species and possibly cell types, but it usually occurs during
75 M or G1 [6-8]. In yeast and mammals, maintenance of centromeric CENP-A depends on CENP-
76 C, the Mis18 complex, and HJURP [9-15]. In *Drosophila*, the Mis18 complex and HJURP are
77 absent, but CAL1 takes on a similar role by interacting with both CENP-C and CID [16-18].
78 CID, CENP-C, and CAL1 rely on each other for loading to maintain centromere identity [10, 16,
79 18, 19].

80 While CENP-C is required for centromere maintenance, it also has a direct role in
81 kinetochore assembly by recruiting MIS12 in mammals [20-22] and *Drosophila* [23-25]. In
82 many organisms, including *Drosophila* and mammals, the kinetochore is loaded once the nuclear
83 envelope breaks down, and is only present during cell division. Although considered part of the
84 inner kinetochore, CENP-C is present throughout the cell cycle. In *Drosophila,* no other
85 kinetochore proteins except for MIS12 exhibit this behavior [26]. CENP-C recruits MIS12 [24,
86 25], and they directly interact to form an inner kinetochore complex that is present throughout
87 the cell cycle [21, 23, 27].
88 Following the pachytene stage of meiosis, mammalian and *Drosophila* oocytes enter a
89 long pause in prophase. If centromere proteins are loaded once per cell cycle, they would have to
90 be maintained for a long time before kinetochores are assembled and cell division commences
91 [28]. Cohesins, for example, are loaded during S-phase and deteriorate with age, causing
92 aneuploidy in older mothers [29, 30]. CENP-A nucleosomes in mouse oocytes are stable and do
93 not need to be maintained during meiotic prophase [28, 31]. Furthermore, CENP-C becomes
94 immobilized at metaphase [32]. Thus, it is possible that the CENP-C loaded along with CENP-A
95 in G1 is sufficient for kinetochore assembly. However, the stability of CENP-C during meiotic
96 prophase has not been tested.
97 In this study, we investigated the meiotic prophase dynamics of CENP-C, CAL1, and
98 CID in *Drosophila* oocytes. As with CENP-A in mouse oocytes [28], we found that CID is stable
99 throughout *Drosophila* oocyte meiotic prophase, and there was little addition of new subunits. In
100 fact, expression of CID during prophase can lead to ectopic kinetochore formation and abnormal
101 chromosome segregation. CAL1 is gradually lost during prophase and is absent in metaphase I
102 oocytes. CENP-C is unique because it is loaded at centromeres using an exchange mechanism

103 during meiotic prophase, and this is required for assembly of the meiotic kinetochore. Thus,

104 CENP-C is loaded independently of centromere maintenance in a process that is required for

105 kinetochore assembly.

106 ## Results

107 **CENP-C, but not CAL1 or CID, loads onto centromeres during prophase I**

108 The analysis of centromere protein dynamics during prophase is facilitated by the
109 organization of the *Drosophila* ovary. Each of the two *Drosophila* ovaries contains several
110 strings, or ovarioles, of oocytes arranged in developmental order (Figure 1A). At the anterior end
111 of each ovariole is the germarium, which includes mitotically dividing cells (region 1) and early
112 meiotic prophase (regions 2-3). Region 3 (stage 1) oocytes leave the germarium and enter the
113 vitellarium. Stages 1 to 13 last 5 days, during which meiosis remains in prophase while the
114 oocyte grows and matures [33, 34]. At the posterior end of the ovariole (stage 13-14), the oocyte
115 enters prometaphase. Meiosis arrests at metaphase I until passage through the oviduct and
116 fertilization occurs.

117 To determine if CENP-C, CAL1, or CID can assemble on chromosomes during meiotic
118 prophase, we used *UASP* regulated EGFP-tagged transgenes. With these transgenes, expression
119 of *Cenp-C, cal1,* and *cid* was induced during female meiotic prophase using one of three GAL4-
120 expressing transgenes (Figure 1A). We started with *P{GAL4::VP16-nos.UTR}CG6325*^{MVD1}
121 (referred to as *MVD1*) because it promotes expression of UAS transgenes through all stages of
122 the germline, including the pre-meiotic cyst cells of the germline and continuing throughout all
123 stages of oocyte development [35]. Crossing each transgene to *MVD1* resulted in CID, CAL1,
124 and CENP-C localization in region 2a and throughout stages 1 to 5 of oogenesis (Figure 1B-D,
125 Figure S 1).

126 As expected, CENP-C regulated by *MVD1* (referred to as *GFP-Cenp-C/MVD1* oocytes)
127 was localized to meiotic centromeres in metaphase I of stage 14 oocytes. In contrast, surprising
128 patterns were observed in stage 14 oocytes when CID or CAL1 were regulated by *MVD1* (Figure

129 1B, D). In *cid-GFP/MVD1* oocytes, CID was present as centromeric foci in about 50% of
130 oocytes (Figure 1E) . In other oocytes, however, CID was present on most of the meiotic
131 chromatin. It was enriched in puncta and appeared to recruit CENP-C to these ectopic sites
132 (Figure S 2). Thus, overexpression of CID in prophase can result in non-centromeric chromatin
133 localization. In contrast, CAL1 was absent from the centromeres in *cal1-GFP/ MVD1* stage 14
134 oocytes, although it was frequently on the spindle (Figure 1D, Figure S 2). The spindle
135 localization appears to be due to overexpression because it was not observed when CAL1 was
136 regulated by its own promoter (Figure S 2). Thus, CAL1 appears to be unloaded from meiotic
137 centromeres during prophase.

138 To test if early prophase loading was sufficient for later stages of meiosis, we used
139 *P{GAL4-nos.NGT}A* (referred to as *NGTA*), which expresses in the germarium, including the
140 mitotic divisions and early meiotic prophase (Figure S 3). Importantly for our study, *NGTA*
141 expression ends in early prophase (stages 3-5). When regulated by *NGTA,* centromeric
142 localization of CID, CAL1, and CENP-C was observed in region 2a and stages 1-5 (Figure 1B,
143 C, Figure S 1). Similar results were observed with *HA-Cenp-C/ NGTA* oocytes (Figure S 4A).
144 These results correspond to the *NGTA* expression pattern. In stage 14 oocytes, considerably after
145 the zone of *NGTA* expression, CID was localized at the centromeres (Figure 1B). These data
146 show that CID loaded during or prior to early meiotic prophase is maintained throughout
147 prophase and into metaphase I of stage 14 oocytes. As with *MVD1,* CAL1 was not detected at
148 centromeres in *cal1-GFP/ NGTA* stage 14 oocytes (Figure S 1), confirming that CAL1 is
149 unloaded during meiotic prophase. While *GFP-Cenp-C/ NGTA* oocytes had centromeric CENP-
150 C localization in stages 1-5 (see above), it was absent in stage 14 oocytes (Figure 1C). These
151 results suggest that CENP-C is unloaded from the centromeres during meiotic prophase.

152 To test if centromere proteins load during meiotic prophase, we used
153 *P{w[+mC]=matalpha4-GAL-VP16}V37* (referred to as *mata*), which begins expression in late
154 prophase (region 2B/3) and continues through metaphase I in the stage 14 oocyte [36, 37]. In
155 *cal1-GFP/ mata* oocytes, a weak GFP signal was frequently observed on the spindle, and rarely
156 at the centromeres (Figure 1D, Figure S 2). This is consistent with the observations made in *cal1-*
157 *GFP/ MVD1* oocytes that CAL1 is absent from metaphase I centromeres. CID induced by *mata*
158 during late prophase I was present on most of the meiotic chromatin in 100% of the oocytes
159 (Figure 1B). This was similar to the pattern observed in some of the *cid-GFP/ MVD1* oocytes;
160 CID was enriched in some puncta, and also appeared to recruit CENP-C and SPC105R to the
161 meiotic chromatin (Figure S 2). Ectopic CID affected chromatin organization, as individual
162 bivalents could be discerned, unlike wildtype metaphase I oocytes in which the chromosomes are
163 assembled in a single karyosome. These females were also sterile, suggesting that overexpression
164 of CID during prophase appears to be deleterious, resulting in CID localizing to most of the
165 chromatin, recruiting other centromere and kinetochore proteins, and causing changes in
166 chromosome organization.
167 CENP-C localized only to the centromeres in *GFP-Cenp-C/ mata* oocytes (Figure 1D,
168 Figure S 4A,B). In addition, heat shock was used to induce a pulse of expression during prophase
169 and resulted in localization of CENP-C (Figure S 4C). These data indicate that CENP-C is
170 recruited to centromeres during meiotic prophase. Thus, meiotic CENP-C dynamics are different
171 than CID and CAL1. CID expression during or prior to early prophase is sufficient for meiosis I.
172 In contrast, CENP-C expression later in prophase is required for its centromere localization in
173 meiosis I.

174 **Centromeric CENP-C exchanges during prophase I**

175 The results with *NGTA* and *mata* used to express *GFP-Cenp-C* suggest that centromeres
176 unload and load CENP-C during meiotic prophase. To test the relationship between the
177 unloading and loading of CENP-C, females were generated that expressed two forms of CENP-C
178 (Figure 2A). *GFP-Cenp-C* was under the control of its own promoter while *HA-Cenp-C* was
179 under the control of *mata*. With these transgenes we could measure if the HA-CENP-C induced
180 in prophase would replace the constitutively expressed GFP-CENP-C. In addition, we knocked
181 down *GFP-Cenp-C* expression in prophase by RNAi using shRNA *GL00409,* which targets a
182 sequence within the 5' UTR of *Cenp-C* and is not present in *HA-Cenp-C*. GFP-CENP-C was
183 expected to be expressed at all stages of the germline but, due to containing the 5' UTR, was
184 sensitive to RNAi in meiotic prophase. In contrast, HA-CENP-C expression would begin in early
185 prophase and be resistant to RNAi because it lacks the 5'UTR. This setup allowed us to
186 determine whether unloading of centromeric CENP-C is dependent on a cytoplasmic pool of
187 CENP-C.

188 In *GFP-Cenp-C*, *HA-Cenp-C* (no RNAi) females, the GFP and HA variants were both
189 maintained (Figure 2B, E). A severe reduction in stage 5 and stage 14 GFP-CENP-C levels was
190 observed in *GFP-Cenp-C*, *HA-Cenp-C*, *GL00409* females (Figure 2C, E). In contrast, the
191 decrease in GFP-CENP-C was less severe in the absence of HA-CENP-C expression (*GFP-*
192 *Cenp-C*, *GL00409* females, Figure 2D, E). To explain these observations, we propose that the
193 unloading of centromeric CENP-C depends on the availability of a replacement. In addition,
194 while the GFP-CENP-C levels at the centromeres drops dramatically in the presence of HA-
195 CENP-C and RNAi, a low level was still observed in stage 14 oocytes (Figure 2D). These results

196 suggest that, although most CENP-C is exchanged during prophase, there is a small pool of
197 CENP-C that is maintained throughout meiosis.

198 **CENP-C regulates centromere clustering, recombination, and MIS12 loading in early**
199 **prophase I**

200 These results show that there is a population of CENP-C loaded during meiotic prophase
201 that is distinct from the population required for the maintenance of CID at the centromeres. To
202 investigate *Cenp*-C function in early prophase, we knocked down its expression by RNAi using
203 an shRNA (*GL00409*) with either the *NGTA* or *MVD1* promoters. Females expressing *GL00409*
204 with *MVD1* (*GL00409*/*MVD1* oocytes) were sterile and agametic [38]. *MVD1*-driven expression
205 in all premeiotic mitotic germ cells and a requirement for CENP-C during these mitotic divisions
206 would explain the agametic phenotype. Thus, the remaining early prophase experiments were
207 performed with females expressing *GL00409* with *NGTA* (*GL00409/NGTA* oocytes).

208 *GL00409/NGTA* females were fertile but displayed a high level of X-chromosome
209 nondisjunction (7%) compared to controls (0.25%) (Table 1). A similar result was observed with
210 a different shRNA targeting *Cenp-C* (*HMJ21500*). Because *NGTA* expression occurs only during
211 early prophase, these results suggest CENP-C has an early meiotic function required for
212 chromosome segregation. To investigate the mechanisms of nondisjunction caused by loss of
213 CENP-C, we characterized processes that occur early in meiotic prophase such as centromere
214 assembly, meiotic recombination, centromere pairing, sister chromatid cohesion, and
215 synaptonemal complex (SC) formation.

216 The intensities of CENP-C and CID at the centromeres were moderately decreased in
217 early prophase nuclei of *GL00409*/*NGTA* oocytes (Figure 3A - C). The mild reduction of both
218 centromere proteins suggests that the knockdown of CENP-C only had a mild effect on

219 centromere maintenance. For another measure of CENP-C function in prophase, we examined
220 the localization of MIS12. In *Drosophila* mitotic cells, CENP-C promotes kinetochore assembly
221 by recruiting MIS12 [23-25]. MIS12-GFP localized to centromeres in control oocytes, starting in
222 region 2a of the germarium (Figure 3D). The intensity of centromeric MIS12-GFP was
223 significantly reduced in *GL00409/NGTA* females (Figure 3E) indicating that CENP-C promotes
224 recruitment of MIS12 during meiotic prophase. These results show that MIS12 localizes to the
225 centromeres in meiotic prophase and depends on CENP-C.
226
227 **Table 1: Fertility, nondisjunction and crossing over in *Cenp-C* RNAi females**

	Fertility	Nondisjunction (NDJ)		Recombination (% of control)			
	Offspring per female (# of females)	Homologous Chromosome NDJ (# of offspring)	Sister Chromatid NDJ (# of offspring)	*st-cu (m.u.)*	*cu-e (m.u.)*	*e-ca (m.u.)*	# of progeny
Control	24.3 (105)	0.25% (1590)	0.5% (2696)	4.4	2.2	29.4	2853
GL00409 / NGTA	10.0 (240)	7.0% (1658)	2.6% (1164)	9.4 (226%)	21.1 (101%)	22.9 (81%)	1668
HMJ21500 / NGTA	3.3 (133)	7.6 (1213)	ND	ND	ND	ND	ND
GL00409 / MVD1	0.27 (105)	0% (54)	- [a]	-	-	-	-

228
229 [a] not enough progeny to accurately measure nondisjunction or crossing over
230
231 Increased frequencies of nondisjunction can be associated with loss of SC and/or a
232 reduction in crossing over (CO) [39]. SC assembly in *GL00409/NGTA* females was normal,
233 indicated by the thread-like appearance of the transverse filament protein C(3)G [40] (Figure S
234 5). We measured the frequency of crossing over in *GL00409/NGTA* females and observed an
235 increase in centromeric crossovers, but overall, crossing over was not decreased (Table 1). When

236 the centromeres were genetically marked (see Methods, Table 1), we observed an increase in
237 sister chromatid nondisjunction. Thus, meiotic nondisjunction may occur because of a cohesion
238 defect, which could be caused by the increase in proximal crossovers [41].

239 A cohesion defect can be observed as an increase in the number of centromere foci [42,
240 43]. Indeed, there was an increased number of CID foci in the germaria of *GL00409/NGTA*
241 ovaries, indicating a separation of centromeres (Figure 3F, G). We tested if the cohesion defect
242 persisted, and therefore would result in increased CID foci in metaphase I oocytes. The
243 variability in CID foci number was greater in the experimental group, but the mean was not
244 significantly different from the control (Figure 3H, I).

245 Because nonhomologous centromeres normally cluster in early prophase, we used
246 chromosome-specific fluorescence in situ hybridization (FISH) probes for the pericentromeric
247 regions of the X and 2nd chromosomes to examine pairing and clustering of the centromeres
248 (Figure 4A). Clustering defects were defined as nuclei containing 3 or more clearly separated
249 probe foci (of any color) whereas control oocytes had 1-2 foci. As with the experiment to detect
250 CID foci, the FISH foci failed to cluster (Figure 4B). Pairing defects were defined as greater than
251 one FISH focus per probe. While homologous centromeres were efficiently paired in wild-type
252 germarium, pairing was defective in *GL00409/NGTA* oocytes (Figure 4C). These results suggest
253 that there are defects in both centromere pairing and clustering, consistent with a defect in sister
254 centromere cohesion.

255 **Prophase CENP-C plays a critical role in maintenance of centromeres and kinetochores.**

256 To test the function of CENP-C loaded during late prophase, we used *mata* to express
257 *Cenp-C* shRNA (*GL00409/mata*). The *GL00409/mata* females were sterile, although this could
258 be due to defects in early embryo mitosis rather than meiosis. To investigate the effects on

259 meiosis I, stage 14 *GL00409/mata* oocytes were analyzed for meiotic defects. The intensity of
260 CENP-C at the centromeres was reduced to approximately 25% of the intensity in control
261 oocytes (Figure 5A, B). The intensity of CID at the centromeres was mildly reduced in
262 *GL00409/mata* oocytes to approximately 80% of control levels (Figure 5A, C). These results
263 suggest that CENP-C might play a role in the stabilization of CID late in meiotic prophase or in
264 metaphase I.

265 To determine if the loss of CENP-C affects kinetochore assembly, we quantified the
266 intensity of MIS12 and SPC105R in mature oocytes. Consistent with the reduction in CENP-C
267 levels, we observed approximately 85% reduction in MIS12 levels and a 90% reduction in
268 SPC105R in *GL00409/mata* oocytes (Figure 5D-G). Consistent with the loss of SPC105R
269 recruitment, we observed an increase in the distance between centromeres and microtubules
270 (Figure S 6), which has previously been observed when SPC105R is depleted [44]. These results
271 suggest CENP-C recruits MIS-12, which then recruits SPC105R, although we can't rule out
272 CENP-C recruits SPC105R directly. We previously showed that loss of SPC105R was associated
273 with loss of sister centromere cohesion [45]. However, we did not observe this phenotype in
274 *GL00409/mata* oocytes (Figure S 6), suggesting sufficient SPC105R remains to protect cohesion.

275 To determine whether the loss of CENP-C in oocytes affected chromosome segregation
276 at meiosis I, we assayed for bi-orientation of homologous chromosomes using FISH. We
277 observed a dramatic increase in bi-orientation errors (primarily mono-orientation) in
278 *GL00409/mata* oocytes (Figure 6A,B), and a decrease in the distance between homologous
279 centromeres, compared to the control (Figure 6C). These spindle attachment errors could indicate
280 that CENP-C plays a direct role in error correction, but more likely has an indirect effect due to
281 the function of CENP-C in kinetochore assembly.

282 **Rescue of the CENP-C phenotype by late prophase expression of a wild-type allele**

283 Prophase-expressed CENP-C can load onto the centromeres and the defects in
284 *GL00409*/*mata* females suggest that prophase CENP-C expression is required for meiosis and
285 fertility. To directly test if prophase-expressed CENP-C is functional in meiosis, we tested if the
286 *HA-Cenp-C* transgene could rescue loss of endogenous *Cenp-C*. The *HA-Cenp-C* transgene lacks
287 the 5'UTR that includes the target sequence for *GL00409,* and therefore, is resistant to
288 knockdown by RNAi. When *HA-Cenp-C* was co-expressed with *GL00409* using *mata* in
289 oocytes, we observed localization of HA-CENP-C to the centromeres and restoration of MIS12
290 and SPC105R localization (Figure 5D-G). In addition, the biorientation defects in *GL00409/mata*
291 oocytes were rescued by expression of HA-CENP-C (Figure 6). Thus, prophase expression of a
292 CENP-C transgene rescued the defects observed in RNAi oocytes.

293 Despite the rescue of the meiotic RNAi phenotypes, however, expression of HA-CENP-C
294 using *mata* caused sterility (Table 2). These results suggest overexpression of CENP-C leads to
295 loss of fertility. The females expressing HA-CENP-C had normal oocytes at metaphase I,
296 making it likely that the defect causing sterility is after meiosis I, possibly during embryonic
297 mitosis. To circumvent the sterility from *mata*-induced expression of *Cenp-C,* we used
298 *P{w[+mC]=osk-GAL4::VP16}A11* (referred to as *oskGal4*). The expression pattern of *oskGal4*
299 is similar to *matα* but at lower levels [46]. Using *oskGal4* to induce *UASP*-regulated *Cenp-C*,
300 either GFP-tagged or HA-tagged, resulted in fertile females (Table 2). We then used *oskGal4* to
301 determine if prophase expression of CENP-C could rescue the phenotype of a hypomorphic
302 allele, *Cenp-C*$^{Z3-4375}$ [47].

303

304 **Table 2: Fertility in *Cenp-C* RNAi, mutant and transgenic females**

Genotype	Offspring per female (# of females)
Control (*w*-)	**22.93 (90)**
HA-Cenp-C ; matα	**0.58 (325)**
HA-Cenp-C ; oskGal4	**23.15 (125)**
GFP-Cenp-C ; matα	**0.14 (150)**
GFP-Cenp-C ; oskGal4	**18.11 (65)**
Cenp-C^{Z}/+	**11.5 (120)**
Cenp-C^{IR35}/+	**13.58 (160)**
Cenp-C^{pr141}/+	**19.82 (105)**
Cenp-C^{Z}/Cenp-C^{Z}	**1.46 (120)**
Cenp-C^{Z}/ Cenp-C^{IR35}	**0.06 (270)**
Cenp-C^{Z}/ Cenp-C^{pr141}	**0.25 (70)**
Cenp-C^{Z}/ Cenp-C^{IR35}; HA-Cenp-C; matα	**1.358 (460)**
Cenp-C^{Z}/ Cenp-C^{IR35}; HA-Cenp-C ; oskGal4	**15.22 (180)**
Cenp-C^{Z}/ Cenp-C^{pr141}; GFP-Cenp-C; matα	**0.21 (125)**
Cenp-C^{Z}/ Cenp-C^{pr141}; GFP-Cenp-C ; oskGal4	**11.27 (130)**
GL00409 ; matα	**0 (120)**
GL00409 ; oskGal4	**10.81 (90)**
GL00409; HA-Cenp-C; matα	**0.08 (430)**
GL00409; HA-Cenp-C; oskGal4	**26.72 (65)**

305

306 When *Cenp-C$^{Z3-4375}$* was heterozygous to a null allele (*Cenp-C^{IR35}*), the females were
307 sterile and centromeric CENP-C levels in oocytes were reduced, though not to the same levels as
308 with *GL00409* (Figure 5A, B). Bi-orientation errors were also elevated in *Cenp-C$^{Z3-4375}$/Cenp-*
309 *C^{IR35}* mutant oocytes, though not to the same extent as the shRNA-expressing oocytes (Figure 6).
310 Expression of HA-CENP-C or GFP-CENP-C using *oskGal4* was found to rescue the sterility of
311 *Cenp-C$^{Z3-4375}$/Cenp-C^{IR35}* mutant females (Table 2). In addition, SPC105R localization was
312 restored (Figure 5F-G) and the biorientation defects in *Cenp-C$^{Z3-4375}$/Cenp-C^{IR35}* mutant females

313 was rescued (Figure 6). These results show that late prophase expression of CENP-C contributes
314 to kinetochore function in meiosis I.

315 **Regulation of CENP-C loading and centromere integrity**

316 The RNAi resistance of the *HA-Cenp-C* transgene can be used to express mutant variants
317 in the absence of wild-type CENP-C. Previous studies have shown that the C-terminal domain of
318 *Drosophila* CENP-C interacts with the centromere components CID and CAL1 [17, 23]. To
319 determine what domains of CENP-C are required for prophase loading in oocytes, we generated
320 two *Cenp-C* transgenes expressing either the N-terminal (aa 1-788, *Cenp-C*^{N}) or C-terminal
321 (789–1411, *Cenp-C*^{C}) domain of CENP-C. The N-terminal domain was not detected by
322 fluorescence microscopy, suggesting it is either unstable or does not localize. In contrast, CENP-
323 C^{C} was loaded to the centromeres during prophase (Figure S 4, Figure S 6), but failed to recruit
324 SPC105R or MIS12 (Figure 5D-G). The CENP-C^{C} protein may have a dominant negative effect
325 because there was a significant reduction of SPC105R localization in *GL00409; Cenp-C*^{C}
326 oocytes compared to *GL00409.* These results support the conclusion that the C-terminal domain
327 of CENP-C is required for centromere localization, while the N-terminal domain recruits MIS12
328 and the rest of the outer kinetochore.

329 Two pathways have been proposed to load CENP-C via the C-terminal domain. The first
330 occurs during anaphase or G1, is required to maintain centromere identity [8, 48], and depends
331 on CAL1 [10]. The second occurs during prophase, may be required to build kinetochores, and
332 depends on CDK1 in mitotic cells [49]. To examine the role of CAL1 in prophase loading, we
333 measured CENP-C loading in *cal1* RNAi oocytes (*GL01832*). Similarly, the same experiment
334 was done using an shRNA (*HMS01531*) to knock down *Cdk1* mRNA. In both experiments, HA-
335 CENP-C was observed in stage 5 oocytes, suggesting neither CAL1 nor CDK1 are required for

336 prophase loading of CENP-C (Figure S 7). We did not examine stage 14 oocytes because, as
337 described above, CAL1 is not present, and *Cdk1* RNAi oocytes fail to enter prometaphase.
338 The *Cenp-C*$^{Z3.4375}$ mutation is in the C-terminal domain and is present at the centromeres
339 in decreased amounts (Figure 5A, B). We also observed a second phenotype suggesting a loss of
340 kinetochore integrity. In some *Cenp-C*$^{Z3.4375}$ mutant oocytes, foci of CENP-C protein were
341 detached from the main chromosome mass and moved towards the poles (Figure 7A, B). This
342 suggests that one of the defects in *Cenp-C*$^{Z3.4375}$ mutant oocytes is a failure to maintain
343 attachment of the kinetochore to the underlying centromeric chromatin. Surprisingly, this
344 phenotype was observed in the presence of a wild-type transgene (Figure 7C). Either the
345 kinetochore phenotype is dominant, or it is due to an early prophase function, and that expression
346 of the transgene, which is in late prophase, was too late to rescue the phenotype.
347 The kinetochore detachment phenotype is reminiscent of results from budding yeast
348 indicating condensins have a role in maintaining the cohesive structure of the centromeres [50,
349 51]. To compare the two phenotypes, we examined centromere and kinetochore protein
350 localization in oocytes depleted of Condensin subunits. Depletion of SMC2 results in severe loss
351 of centromere integrity (20/22 oocytes, Figure 7E). In contrast to *Cenp-C*$^{Z3.4375}$ mutant oocytes,
352 CID was stretched towards the poles in addition to CENP-C. A similar, although less severe,
353 phenotype was observed in *gluon* (SMC1) RNAi oocytes (5/11 oocytes), which could be due to a
354 weaker knockdown. RNAi against subunits specific for Condensin I (Barren/Cap-H, 0/11) or
355 Condensin II (CapH2, 0/6) did not have this phenotype, although we can't rule out the possibility
356 that the absence of a phenotype was due to insufficient mRNA knockdown (Figure 7F).
357 SPC105R was also stretched towards the poles (Figure 7G), and a similar phenotype was
358 observed using *Top2* RNAi (7/7, Figure 7H)), as observed previously [52]. These results show

359 the importance of two mechanisms that resist the pulling forces on the kinetochores and keep the
360 centromere and kinetochore together: Condensin /Top II maintains the compact centromeric
361 chromatin while the C-terminal domain of CENP-C maintains the connection between
362 centromeric chromatin and the inner kinetochore.

363 ## Discussion

364 **Prophase dynamics of centromere proteins in oocytes**

365 In *Drosophila*, centromere maintenance involves three proteins, CID, CAL1, and CENP-
366 C, and occurs during late M or G1 (see Introduction). We show here that CENP-C must be
367 loaded during meiotic prophase for centromere clustering, cohesion, and normal kinetochore
368 assembly. We observed increased CENP-C unloading when there was a cytoplasmic source of
369 CENP-C for replacement. This indicates that CENP-C dynamics involves an exchange
370 mechanism, and without new sources of CENP-C, the dynamics are reduced. In contrast to
371 CENP-C, expression of CID in premeiotic cells or early prophase was sufficient for robust
372 localization in metaphase I. Surprisingly, CAL1 is unloaded during prophase and absent in
373 metaphase I, which is in contrast to observations in mitotic cells [7, 16]. Compared to CID or
374 CAL1, CENP-C is unique in requiring prophase loading for its functions in meiosis.

375 The stable property of CID is consistent with studies on CENP-A in mouse oocytes [28].
376 It has been reported, based on changes in fluorescence intensity, that CID is incorporated during
377 meiotic prophase of *Drosophila* females [48]. These results do not conflict with ours, as we did
378 observe small decreases in CID levels when CENP-C was depleted. However, the significance of
379 this small amount of CID prophase loading is not known. In contrast, overexpression of CID
380 during meiotic prophase resulted in ectopic localization to most of the chromatin, recruitment of
381 kinetochore proteins like CENP-C and SPC105R, and sterility. Similar observations of ectopic
382 localization have been made when CID is overexpressed in somatic cells [53-55]. Thus, it may
383 be important to limit CID expression during prophase to avoid localization to non-centromeric
384 locations.

385 The C-terminal domain of CENP-C had similar dynamic properties during prophase as
386 the full-length protein. This part of the protein also contains the elements required to interact
387 with CID and CAL1 for centromere maintenance [17, 18, 25]. Thus, CENP-C prophase loading
388 may involve recruitment to existing sites containing CID. Some evidence in mammals, however,
389 suggests CENP-C has both CENP-A-dependent and independent localization mechanisms,
390 although in most of these studies, loading during G2 is not specifically addressed [56]. CDK1
391 has been implicated in CENP-C dynamics in chicken and human cells [49], although we did not
392 see an effect on CENP-C loading when CDK1 was depleted in *Drosophila* oocytes. Further work
393 is need to understand what regulates CENP-C dynamics during prophase.

394 **Early prophase function: centromere clustering and cohesion**

395 When CENP-C was depleted from early prophase oocytes, we observed an increased
396 number of centromere foci. Our results suggest the increased CID foci phenotype could be due to
397 a loss of centromeric cohesion because we also observed an increase in sister chromatid
398 nondisjunction. These observations are consistent with and extend prior studies on *Cenp-C* [47].
399 These authors also found that *Cenp-C*$^{Z3\text{-}4375}$ mutant females had defects in centromere clustering
400 in pachytene oocytes (region 3 of the germarium). The centromere clustering and pairing
401 phenotypes are similar to a hypomorphic allele of replication protein *mcm5* that was associated
402 with loss of SMC1 at the centromeres [57]. Thus, we propose that CENP-C is required to recruit
403 or maintain cohesion. A recruitment function of CENP-C could occur when cohesion is
404 established in S-phase [42]. Alternatively, our results show striking similarities to the known
405 roles of mammalian and yeast CENP-C in recruiting Moa1 or Meikin [58, 59], which are
406 protectors of centromeric cohesion and particularly important for meiosis I.

407 **Late prophase function: kinetochore assembly**

408 Depletion of prophase CENP-C resulted in phenotypes associated with loss of the
409 kinetochore. This includes loss of MIS12 and SPC105R when CENP-C was depleted in
410 prophase. These results show that CENP-C is required for most or all kinetochore assembly,
411 consistent with studies in *Drosophila* mitotic cells [19, 24, 25]. These results also show that
412 unlike CID/CENP-A, CENP-C loaded prior to prophase, that is required for centromere
413 maintenance, is not sufficient for kinetochore assembly. Why CENP-C is loaded during prophase
414 instead of prometaphase I like most other kinetochore proteins is not known. Studies in
415 vertebrate cells have shown that CENP-C is dynamic during interphase but stable in metaphase
416 [32, 60]. In addition, CENP-C turnover is much slower compared to microtubules and
417 kinetochore proteins [61]. Therefore, it may be necessary to assemble CENP-C at the
418 centromeres during prophase for two reasons: it is not stably maintained like CID and its
419 dynamics are much slower than other spindle proteins. Prophase loading may also provide a
420 stable and defined platform for kinetochore assembly at the beginning of meiotic prometaphase
421 in oocytes.

422 The C-terminal domain of CENP-C was recruited to the centromeres but failed to
423 assemble a kinetochore. Thus, the N-terminal domain of CENP-C appears to interact with MIS12
424 and recruit the rest of the kinetochore, consistent with previous studies in *Drosophila* [23, 27].
425 The *Cencp-C*$^{Z3\text{-}4375}$ mutation, which causes a substitution of amino acid 1115 [47], apparently
426 weakens the interaction between CENP-C and the centromere. This is likely the cause of the
427 detached kinetochore phenotype in this mutant, which indicates a failure to maintain kinetochore
428 integrity when experiencing the force of microtubule pulling. We have also shown that
429 Condensin, along with Topoisomerase II [52], is required to maintain the integrity of CENP-C

430 and other kinetochore proteins on the chromosomes. Previous work in yeast has suggested that
431 condensins have a role in maintaining the cohesive structure of the centromeres in metaphase
432 [50, 51].

433 **Implications of CENP-C prophase loading**

434 CENP-A/CID is remarkably stable [62, 63], not needing to be loaded during the extended
435 prophase in oocytes. Our overexpression of CID results suggests that preventing CID from
436 loading in prophase may be necessary to maintain a single centromere on each chromosome. In
437 contrast, CENP-C must be loaded during prophase. Why CENP-C is not like CENP-A/CID and
438 must be loaded during prophase is not known. It is possible that more CENP-C is needed for
439 kinetochore assembly than centromere maintenance. It may simply be that, for unknown reasons,
440 CENP-C is not as stable as CENP-A, and therefore requires replenishment to maintain its levels.
441 Regardless of the reason, the requirement for CENP-C prophase loading could affect the health
442 of aging oocytes. If loading of CENP-C is compromised in oocytes that have spent a longer time
443 in meiotic prophase, our results show that sister chromatid cohesion, kinetochore assembly, and
444 meiotic chromosomes segregation could be defective, leading to higher levels of aneuploidy.
445

446 ## Acknowledgements

447 We thank Marina Druzhinina for technical assistance, Christian Lehner for providing
448 Drosophila stocks and antibodies. We also thank Sarah Radford for early work on this project.
449 We thank the Bloomington *Drosophila* Stock Center (NIH P40OD018537) and the TRiP project
450 at Harvard Medical School for providing fly stocks used in this study. J.F was supported by a
451 NIH IRACDA post-doctoral Fellowship. This work was supported by NIH grant GM101955 to
452 K.S.M.

453 ## Materials and Methods

454 ### *Drosophila* strains and genetics

455 *Drosophila* crosses and stocks were kept at 25°C on standard medium. Fly stocks,
456 including lines expressing a short hairpin RNA (shRNA), were obtained from the Bloomington
457 Stock Center or the Transgenic RNAi Project at Harvard Medical School [TRiP, Boston, MA,
458 USA, flyrnai.org]. Information about the genetic loci can be found on FlyBase [flybase.org].
459 *Drosophila* were obtained from the Bloomington Stock Center. Expression of the shRNA was
460 controlled by the Upstream Activating Sequence (UAS), which is activated by expression of
461 GAL4 under the control of a tissue-specific enhancer [1]. Five *Gal4* strains were used in this
462 study, four of which were germline-specific: *P{matalpha4-GAL-VP16}V37* and *P{w[+mC]=osk-*
463 *GAL4::VP16}A11* promote expression after zygotene, *P{GAL4-nos.NGT}A* promotes expression
464 only in the germarium (during prophase I), and *P{GAL4: :VP16-nos.UTR}CG6325*^{MVD1} promotes
465 expression throughout the whole germline. In addition, heat shock was used to induce expression
466 of transgenes using *P{GAL4-Hsp70,PB}89-2-1.*

467 The shRNA used to reduce *Cenp-C* expression, *GL00409*, is located on chromosome II.
468 To measure the extent of the *Cenp-C mRNA* knockdown, total RNA was extracted from stage 14
469 oocytes expressing *GL00409* with *P{matalpha4-GAL-VP16}V37* using the TRIzol Reagent (Life
470 Technologies). cDNA was made using the High-Capacity cDNA Reverse Transcription kit
471 (Applied Biosystems). TaqMan Gene Expression Assays (Life Technologies) were used to
472 measure expression levels of CENP-C. RT-qPCR was done on a StepOnePlus (Life
473 Technologies) real-time PCR system and results showed that the *Cenp-C* RNAi expressed only
474 4% of wild-type RNA. In addition, CAL1 was knocked down using shRNA *GL01832* and CDK1
475 was knocked down using shRNA *HMS01531*, both located on chromosome II. Both shRNAs

476 were sterile in combination with *P{matalpha4-GAL-VP16}V37* and *HMS01531* oocytes failed to
477 enter meiosis I.

478 *Cencp-C*$^{Z3-4375}$ is a homozygous-viable allele that has a missense mutation in the CENP-C
479 motif, changing a proline amino acid to a serine at position 1116 [47]. For the analysis of *Cenp-*
480 *C*$^{Z3-4375}$, trans heterozygous mutant strains were used, with one chromosome carrying either the
481 *Cenp-C*^{IR35} or *Cenp-C*^{pr141} mutation. The *Cenp-C*^{IR35} mutation is a premature stop codon at
482 position 858 before the CENP-C motif and Cupin domain, resulting in a deletion of these regions
483 [64]. The *Cenp-C*^{pr141} mutation is a premature stop codon at position 1107 within the CENP-C
484 motif [64], resulting in a partial deletion of the CENP-C motif and the rest of the protein.

485 **HA- and GFP-tagged transgenes**

486 The coding region of cDNA clone FI18815 was PCR amplified and cloned in frame into
487 pENTR4 (HiFi assembly, NEB) and then into pPHW using Clonase (Life Tech.). The target
488 sequence for *GL00409* is located in the 5'UTR of *Cenp-C* and, therefore, this transgene is RNAi
489 resistant. The GFP-CENP-C transgenes were constructed by Christian Lehner and contain the
490 5'UTR sequences upstream of the GFP sequence, and thus is RNAi sensitive. MIS12 localization
491 was observed using a UASP regulated GFP-fusion transgene [65].

492

493 **Fertility trials, nondisjunction, and crossover assays**

494 The *GL00409 Cenp-C* shRNA was tested for fertility and chromosome segregation errors
495 by crossing females expressing the shRNA to *yw/ B*^{S} *Y* males. The aneuploid genotypes that
496 survive are *y/y/ B*^{S} *Y* (Bar-eyed females) and *y w / 0* (wild-type males). Because half the
497 aneuploid progeny have lethal genotypes, aneuploidy was calculated by multiplying the number
498 of aneuploid progeny by two and dividing by the total number of progeny.

499 Sister chromatid aneuploidy was tested by crossing *y w/ Bwinscy* females expressing the
500 shRNA to *v f B ^ Y* males. If aneuploidy occurs among homologous chromosomes, the expected
501 genotypes that survive are *y w/Bwinscy* and *O/ v f B ^ Y*. Aneuploidy among sister chromatids is
502 detected by the genotypes *y w/y w* (non-bar-eyed females) or *Bwinscy/Bwinscy* (Bar-eyed
503 females). Because the O/ *v f B ^ Y* genotype arises from both MI or MII nondisjunction, only the
504 *y w/y w* and *Bwinscy/Bwinscy* progeny were used to determine the sister chromatid aneuploidy
505 frequency. Therefore, the number of aneuploid progeny counted was multiplied by four and
506 divided by the total number of progeny in order to measure sister chromatid aneuploidy.
507 In order to observe the role of CENP-C in crossing over, females were generated that
508 expressed the shRNA and were heterozygous for four genetic markers on chromosome III: *st, cu,*
509 *e* and *ca*. These females were crossed to a strain carrying all the recessive traits and the
510 frequency of the recombinants was scored.
511
512 **Cytology and immunofluorescence of early prophase oocytes**
513 For immunolocalization experiments in the germaria, mated females were aged for 1-2
514 days at 25°C. In one well of a two well plate, 10-15 ovaries were dissected using 1x Robb's
515 media and then were transferred to the second well containing fresh media. A tungsten needle
516 was used to break open the ovary sheath and tease the ovarioles apart. The dissected ovaries
517 were transferred to a 1.5 mL Eppendorf tube with 4% formaldehyde in 500 ul of Buffer A as
518 described [66]. The ovaries were nutated at room temperature for 10 minutes, then were washed
519 four times before adding the primary antibodies. The next day, following four washes, secondary
520 antibodies were added and incubated at room temperature for 4 hours.

521 **Cytology and immunofluorescence of metaphase I oocytes**

522 For immunolocalization experiments in pro-metaphase I oocytes (stages 13-14), we used
523 the immunocytochemical protocol as described [67]. In brief, 100-200 females were aged 2-3
524 days with males in yeasted vials [68]. Oocytes were collected by pulsing the females in a blender
525 and then separating the oocytes from the bulk fly tissues using a mesh. Oocytes were fixed in 5%
526 formaldehyde solution for 2.5 minutes, and then equal amounts of heptane were added and the
527 oocytes were vortexed for 30 seconds. The membranes were removed by rolling the oocytes
528 between a coverslip and the frosted part of a glass slide. These oocytes were incubated in
529 PBS/1% Triton X-100 for two hours, then washed in PBS/0.05% Triton X-100. The oocytes
530 were blocked in PBS/0.1% Tween 20/0.5% BSA (PTB) for one hour, and then incubated with
531 primary antibodies overnight. Oocytes were washed the next day in PTB and incubated with
532 secondary antibodies for 4 hours at room temperature.

533 Tissues were mounted for confocal imaging using SlowFade Gold (Invitrogen). A Leica
534 TPS SP8 confocal microscope with a 63X, N.A. 1.4 lens was used to visualize fluorescent tags
535 using different colored lasers. Images were imaged by collecting sections throughout the
536 germarium or stage 14 oocyte spindle, using parameters optimized by the Leica Confocal
537 software based on the lens and wavelength. Images were analyzed as image stacks and presented
538 as maximum projections of whole germarium, cells, or spindles.

539 **Antibodies**

540 An antibody against CENP-C made in guinea pig was made by generating a clone
541 expressing amino acids 502-939 (Genscript). This guinea pig anti-CENP-C was used at 1:1000.
542 Additional primary antibodies were rat anti-CID (Active motif, 1:100), rabbit anti-CID (Active
543 motif, 1:100), rabbit anti-SPC105R (1:4000) [69], rabbit anti-GFP (Invitrogen, 1:400), rat anti-

544 HA (Roche, 1:50), mouse anti-C(3)G (1:500) [70], two mouse anti-ORB antibodies, 6H4 and
545 4H8 (1:100 for each) [71] and mouse anti-α tubulin DM1A conjugated directly to FITC (Sigma,
546 1:50). The secondary antibodies that were used were Cy3, Alexa 546, Alexa 633, or Alexa 647
547 from Jackson Immunoresearch Laboratories, and Alexa 488 from Invitrogen. The oocytes were
548 stained with Hoechst 33342 at 1:10,000 (10 μg/ml). FISH probes were obtained from IDT where
549 the X359 repeat was labeled with Alexa 594, the dodeca repeat was labeled with Cy5, and the
550 AACAC repeat was labeled with Cy3.
551

552 **Quantification and statistical analysis**

553 Aneuploidy in flies expressing the *Cenp-C* shRNA with NGTA was compared to that of
554 the control group and a t-test was done to determine if the difference is statistically significant
555 (p-value < 0.05). Sister chromatid aneuploidy in flies expressing the *Cenp-C* shRNA with NGTA
556 was compared to that of the control group and a t-test was used to determine whether the
557 difference was statistically significant (p-value < 0.05). The percent of crossovers at each
558 position was compared to that of the control group using a t-test, and if the difference was
559 statistically significant (p-value < 0.05), then this indicated that elevated or reduced
560 recombination occurred at that specific location.

561 Quantification of CID foci and protein localization in both the germarium and in stage 14
562 oocytes was measured using the Imaris Software. To quantify centromere foci, the automated
563 spots detection feature of Imaris was used. A spot with a XY diameter of 0.20 μm, a Z diameter
564 of 1.00 μm, and a physical interaction with the DNA was counted as a centromere. A t-test was
565 done to compare the number of centromere foci in flies expressing the knockdown to the number
566 in the control group using a p-value < 0.05 to indicate statistical significance.

567 To measure the localization of proteins to the centromere or the nucleus in *Cenp-C*
568 RNAi, intensity experiments were performed using Imaris. The Imaris software was utilized to
569 measure protein intensity at the centromere of the oocyte, using CID as the centromere marker.
570 Spots were chosen in random somatic cells to quantify the intensity of the background. The
571 intensity of the protein at the centromere was divided by the background and a t-test was used to
572 determine whether the centromere protein intensity was reduced with a loss of CENP-C.
573 Intensity experiments were also performed to measure localization of MIS12, SPC105R,
574 or CENP-C to the centromere at stage 14 using a similar protocol. However, background
575 intensity was measured in the oocyte cytoplasm as opposed to measuring the background in the
576 somatic cells for germarium images. A t-test was used to determine whether the intensity of the
577 protein of interest at the centromere normalized to the background was reduced with a loss of
578 CENP-C using a p-value <0.05 to indicate statistical significance.

579 **Figure Legends**

580 Figure 1: **Loading of centromere proteins during meiotic prophase in oocytes. A)** Oocytes
581 are generated and enter meiotic prophase in the germarium. Region 1 contains the stem cell niche
582 as well as the pre-meiotic cyst cells undergoing mitosis. Prophase I of meiosis begins in region
583 2A. Time points are relative to the onset of meiosis [33, 34]. Region 3 is also known as
584 vitellarium stage 1, and at this stage, a single oocyte (orange) has been determined. *NGTA* begins
585 expressing in the mitotic germline (region 1) and ends in region 3 or early in the vitellarium.
586 *MVD1* expression begins earlier than *NGTA,* being expressed in all the mitotic and meiotic
587 stages of the germline, including the stem cells. *Mata* begins expressing in region 2B or 3 and
588 continues until stage 14, the metaphase I-arrested oocyte [36]. **B)** Localization of GFP-tagged
589 CID (green) and centromeres detected using a CENP-C antibody (red). **C)** Localization of GFP-
590 tagged CENP-C, with the centromeres detected using a CID antibody (red). **D)** Localization of
591 GFP-tagged CAL1 (green) with the centromeres detected using a CENP-C antibody (red). In all
592 images, the DNA is blue and the scale bars are 5 um. **E)** Summary of CID, CENP-C, and CAL1
593 localization in Stage 14 oocytes (n = 34, 18, 11, 12, 10, 30, 15, 26, 4).
594

595 Figure 2: **CENP-C is exchanged at the centromeres during meiotic prophase.**
596 Immunocytology was performed on oocytes ubiquitously expressing GFP-CENP-C (green), plus
597 or minus *GL00409* (*Cenp-C*^{RNAi}), and HA-CENP-C (red) using the *mata* promoter. All scale bars
598 represent 5 um and DNA is blue. **A)** *GL00409* recognizes a sequence in the 5' UTR, and,
599 therefore, degrades *GFP-Cenp-C* but not *HA-Cenp-C*. Images show stages 1, 5 and 14 with (**B)**
600 expression of GFP-CENP-C and HA-CENP-C, **(C)** expression of GFP-CENP-C, *Cenp-C*^{RNAi},
601 and HA-CENP-C, and (**D)** expression of GFP-CENP-C with *Cenp-C*^{RNAi}. **E)** The relative

602 intensity of GFP-CENP-C was measured at each stage in each genotype (n = 70, 117, 28, 23; 12,
603 19, 104, 156; 50) with error bars showing standard deviation. For each genotype, the intensity
604 between stage 1 and stage 14 was compared using an unpaired t-test (***p = 0.001;
605 ****p<0.0001).
606
607 Figure 3: **Early Prophase I defects when CENP-C is depleted using NGTA.** Immunocytology
608 was performed on *GL00409/NGTA* oocytes with CID (red), DNA (blue), and scale bars represent
609 5 um. **A)** Region 2 oocytes showing CENP-C in green. **B-C)** The intensities of CENP-C and CID
610 in region 2 were measured in *Cenp-C* RNAi and control oocytes (For B, n = 104 and 88; for C, n
611 = 104 and 87). **D)** Region 2 oocytes with MIS12-GFP in green. **E)** MIS12 intensity was
612 measured in region 2 (n = 13 and 30). **F)** CID foci in *Cenp-C* RNAi region 3 oocytes, with
613 CENP-C in green. **G)** Number of centromere foci was measured based on CID foci in contact
614 with the DNA (n = 84 and 27). **H)** Tubulin (green) and CID foci (red) in *Cenp-C* RNAi
615 metaphase I oocytes. **I)** There was no increase in CID foci observed in stage 14 oocytes (n = 40
616 and 52). Error bars represent standard deviation from the mean. ****p<0.0001
617
618 Figure 4 : **CENP-C is required for centromere pairing and clustering. A)** FISH probes were
619 used to detect the pericentromeric regions of chromosome 2 (red), and X (magenta) in the
620 germarium of *GL00409/NGTA* or control oocytes. DNA is in blue. **B)** Clustering defects were
621 defined as nuclei with greater than 2 of any centromere foci (control n = 16, 20, 14; RNAi n =
622 42, 38, 18). **C)** Pairing defects were defined as oocytes with greater than one focus for a
623 chromosome in a nucleus. Scale bars represent 5 µm and error bars show standard deviation. * =
624 0.0196>p>0.0238, ****p<0.0001.

625

626 Figure 5: **CENP-C is required for kinetochore assembly and chromosome segregation.**
627 Immunocytology was performed on stage 14 oocytes expressing the *GL00409* with *mata*
628 (referred to as *Cenp-C*^{RNAi}) or heterozygous for *Cenp-C* mutations (*Cenp-C*$^{Z3-4375}$/*Cenp-C*^{IR35}
629 referred to as "*Cenp-C*^{Z}"). HA-tagged *Cenp-C* transgenes were coexpressed using the *mata*
630 promoter in RNAi experiments or *osk-Gal4* in *Cenp-C*^{Z} experiments. DNA is in blue and scale
631 bars represent 5 um in all images. **A)** Oocytes with CENP-C (green) and CID (red). **B)** The
632 intensity of CENP-C was measured relative to background (n = 55, 67, 54). **C)** The intensity of
633 CID was measured relative to background (n = 186, 221, 54). **D)** Oocytes expressing MIS12-
634 GFP (green) and CID (red). **E)** Mis12-GFP localization was measured relative to the background
635 (n = 57, 41, 47, 67). **F)** Oocytes with SPC105R (green) and CID (red). **G)** Intensity of SPC105R
636 was measured relative to background (n = 108, 136, 115, 132, 245, 150). *p = 0.0379, **p =
637 0.0086, *** = 0.0002>p>0.0001, ****p<0.0001
638

639 **Figure 6**

640 **Prophase-loaded CENP-C is required for bi-orientation in meiosis I. A)** FISH probes were
641 used to detect the pericentromeric regions of chromosome 2 (red), 3 (grey), and X (magenta).
642 Stage 14 oocytes were *Cenp-C*$^{Z3-4375}$/*Cenp-C*^{IR35} (*Cenp-C*^{Z}) or *GL00409/mata* (*Cenp-C*^{RNAi}). In
643 some cases, *HA-Cenp-C* was expressed using *mata* in *Cenp-C*^{RNAi} experiments or *oskGal4* in
644 *Cenp-C*^{Z} experiments. **B)** Bi-orientation defects were defined as two foci of the same probe that
645 were on the same side of the spindle midzone or only a single focus, indicating mono-orientation
646 (n = 75, 59, 53, 58, 56, 60). **C)** The distance between the center mass of two foci of the same
647 probe, which measures the separation of homologous chromosomes towards opposite poles (n =

648 90, 156, 60, 60, 192, 72). All scale bars represent 5 um and error bars represent standard
649 deviation from the mean. * = 0.0473>p>0.0387, **p = 0.0024, *** = 0.0002 >p> 0.001,
650 ****p<0.001.
651
652 Figure 7 : **Kinetochore detachment in *Cenp-C*$^{Z4.4375}$ mutant oocytes**. A-C) Kinetochore
653 detachment in oocytes, with CENP-C in red, CID in magenta, microtubules in green, and DNA
654 in blue. CENP-C foci have separated from the chromosomes (examples shown with arrows),
655 while the CID remains chromatin associated. Shown are (A) wild-type control, (B) *Cenp-C*$^{Z3.4375}$
656 $^{/}$ *Cenp-C*^{IR35} (labelled *Cenp-C*^{Z}), and (C) *HA-Cenp-C* transgene co-expressed in *Cenp-C*$^{Z3.4375/}$
657 *Cenp-C* ^{pr141} mutant oocytes. D) The distance between the center of the kinetochore focus and
658 the nearest surface of the DNA was measured. All scale bars represent 5 um and error bars
659 represent standard deviation from the mean. (Control n=164 centromeres, *Cenp-C*$^{Z3.4375/}$ *Cenp-*
660 *C*^{IR35} n=284, *Cenp-C*$^{Z3.4375/}$ *Cenp-C*^{IR35}*; HA-CENP-C* n=96). ****p<0.0001. D-E) Requirement
661 of Condensin for kinetochore integrity. *CAPH2* or *SMC2* RNAi oocytes with CID (white),
662 INCENP (red), tubulin (green), and DNA (blue). F-G) *SMC2* or *Top2* RNAi oocytes with
663 SPC105R (white), CENP-C (red), tubulin (green), and DNA (blue). Scale bars represent 5 um.
664

665 **Supplementary Figures**

666

667 Figure S 1: **CAL1 and CID localization in oocytes**. A) Localization of GFP-CID (green) and
668 centromeres detected using a CENP-C antibody (red). B) Localization of GFP-CAL1 (green)
669 with the centromeres detected using a CID antibody (red). (D) Localization of GFP-CENP-C,
670 with the centromeres detected using a CID antibody (red). In all images, the DNA is blue and the
671 scale bars are 5 mm.

672

673 Figure S 2: **GFP-CENP-C, CID-GFP or CAL1-GFP in stage 14 oocytes.** The DNA is blue,
674 microtubules in white, and the scale bars represent 5 um. **A)** Localization of CID-GFP or CAL1-
675 GFP (green) using the *MVD1, mata* or *NGTA*. In the one image (*gcal1-GFP)*, CAL1-GFP is
676 regulated by the endogenous *cal1* promoter. The centromeres were detected using CENP-C (red).
677 **B)** Localization of CID-GFP or GFP-CENP-C (green) using *mata*. The kinetochores were
678 detected using an antibody against SPC105R (red).

679

680 Figure S 3: Expression pattern of NGTA. The expression pattern of **(A)** *P{GAL4-nos.NGT}* and
681 **(B)** *P{GAL4::VP16-nos.UTR}CG6325MVD1* using *UASP-β-galactosidase* as a reporter.
682 Arrowheads indicate anterior tip of the ovariole, where the germarium is located, and the blue
683 stain indicates where each GAL4 promotes expression.

684

685 Figure S 4: Loading of HA-CENP-C during oocyte meiotic prophase. In all images, HA-CENP-
686 C is green, the centromeres are marked with CID (red), and DNA is in blue. The scale bars
687 represent 5 um. **A)** Whole germarium with HA-tagged CENP-C expressed using *NGTA* or *mata*.
688 ORB (white) is enriched in the oocyte. **B)** HA-tagged CENP-C or CENP-C^C was expressed using

689 *mata*. **C)** HA-CENP-C was expressed using *hsp70-Gal4*. Oocytes were collected and fixed after
690 6 hours (early prophase) or 5 hours (stage 14) after a 1-hour incubation at 37°C.
691
692 Figure S 5: SC assembly when CENP-C is depleted in prophase. Confocal images of the
693 germarium with *Cenp-C* RNAi (HMS01171) with (A) no *GAL4* and (B) *NGTA*. DNA is shown
694 in blue, CENP-C is in red, and C(3)G is in green. The scale bar is 10 µm. CENP-C and C(3)G
695 are shown in white in the single channel images. Region 1 of the germarium has been boxed to
696 show increased centromeric C(3)G. The insets show single nuclei from region 1 in the
697 germarium to show co-localization of CENP-C and C(3)G (Scale bar= 3 µm).
698
699 Figure S 6: Additional images of CENP-C localization in RNAi and transgenic oocytes. **A)**
700 *Cenp-C* RNAi or *Cenp-C*^{Z} oocytes with CENP-C (green) and CID (red). **B)** *Cenp-C* RNAi or
701 *Cenp-C*^{Z} oocytes expressing a *Cenp-C* transgene, with HA in red and SPC105R in green, DNA
702 in blue, microtubules in white, and the scale bars represent 5 um. **C)** Oocytes shown in panels A
703 and B were assessed for KT-MT attachments. This was done by measuring the distance between
704 each centromere and the nearest microtubule. **D)** Number of centromere foci was measured
705 based on CID foci in *Cenp-C* RNAi metaphase I oocytes (n = 19 and 36). Error bars represent
706 standard deviation.
707
708 Figure S 7: Loading during prophase does not depend on CDK1 or CAL1. Localization of HA-
709 CENP-C in stage 5 oocytes of **(A)** *cdk1* and **(B)** *cal1* RNAi oocytes. HA is in red, CID is in
710 white, cytoplasmic ORB protein is in green, and DNA is in blue. The scale bar represents 5 um.
711 **C)** Relative intensity of CENP-C in control and RNAi oocytes (n=10, 12, 11).

712 # References

713 1. Nechemia-Arbely Y, Fachinetti D, Cleveland DW. Replicating centromeric chromatin: spatial and
714 temporal control of CENP-A assembly. Exp Cell Res. 2012;318(12):1353-60. Epub 2012/05/09. doi:
715 10.1016/j.yexcr.2012.04.007. PubMed PMID: 22561213; PubMed Central PMCID: PMCPMC3616609.
716 2. Swartz SZ, McKay LS, Su KC, Bury L, Padeganeh A, Maddox PS, et al. Quiescent Cells Actively
717 Replenish CENP-A Nucleosomes to Maintain Centromere Identity and Proliferative Potential. Dev Cell.
718 2019;51(1):35-48.e7. Epub 2019/08/20. doi: 10.1016/j.devcel.2019.07.016. PubMed PMID: 31422918;
719 PubMed Central PMCID: PMCPMC6783363.
720 3. Kixmoeller K, Allu PK, Black BE. The centromere comes into focus: from CENP-A nucleosomes to
721 kinetochore connections with the spindle. Open Biol. 2020;10(6):200051. Epub 2020/06/10. doi:
722 10.1098/rsob.200051. PubMed PMID: 32516549; PubMed Central PMCID: PMCPMC7333888.
723 4. Rosin LF, Mellone BG. Centromeres Drive a Hard Bargain. Trends Genet. 2017;33(2):101-17.
724 Epub 2017/01/11. doi: 10.1016/j.tig.2016.12.001. PubMed PMID: 28069312; PubMed Central PMCID:
725 PMCPMC5467322.
726 5. Sridhar S, Fukagawa T. Kinetochore Architecture Employs Diverse Linker Strategies Across
727 Evolution. Front Cell Dev Biol. 2022;10:862637. Epub 2022/07/09. doi: 10.3389/fcell.2022.862637.
728 PubMed PMID: 35800888; PubMed Central PMCID: PMCPMC9252888.
729 6. Jansen LE, Black BE, Foltz DR, Cleveland DW. Propagation of centromeric chromatin requires exit
730 from mitosis. J Cell Biol. 2007;176(6):795-805. doi: 10.1083/jcb.200701066. PubMed PMID: 17339380;
731 PubMed Central PMCID: PMCPMC2064054.
732 7. Mellone BG, Grive KJ, Shteyn V, Bowers SR, Oderberg I, Karpen GH. Assembly of Drosophila
733 centromeric chromatin proteins during mitosis. PLoS Genet. 2011;7(5):e1002068. doi:
734 10.1371/journal.pgen.1002068. PubMed PMID: 21589899; PubMed Central PMCID: PMCPMC3093364.
735 8. Schuh M, Lehner CF, Heidmann S. Incorporation of Drosophila CID/CENP-A and CENP-C into
736 centromeres during early embryonic anaphase. Curr Biol. 2007;17(3):237-43. PubMed PMID: 17222555.
737 9. Camahort R, Li B, Florens L, Swanson SK, Washburn MP, Gerton JL. Scm3 is essential to recruit
738 the histone h3 variant cse4 to centromeres and to maintain a functional kinetochore. Molecular cell.
739 2007;26(6):853-65. Epub 2007/06/16. doi: 10.1016/j.molcel.2007.05.013. PubMed PMID: 17569568.
740 10. Chen CC, Dechassa ML, Bettini E, Ledoux MB, Belisario C, Heun P, et al. CAL1 is the Drosophila
741 CENP-A assembly factor. J Cell Biol. 2014;204(3):313-29. doi: 10.1083/jcb.201305036. PubMed PMID:
742 24469636; PubMed Central PMCID: PMCPMC3912524.
743 11. Foltz DR, Jansen LE, Bailey AO, Yates JR, 3rd, Bassett EA, Wood S, et al. Centromere-specific
744 assembly of CENP-a nucleosomes is mediated by HJURP. Cell. 2009;137(3):472-84. Epub 2009/05/05.
745 doi: 10.1016/j.cell.2009.02.039. PubMed PMID: 19410544; PubMed Central PMCID: PMCPMC2747366.
746 12. Williams JS, Hayashi T, Yanagida M, Russell P. Fission yeast Scm3 mediates stable assembly of
747 Cnp1/CENP-A into centromeric chromatin. Mol Cell. 2009;33(3):287-98. doi:
748 10.1016/j.molcel.2009.01.017. PubMed PMID: 19217403; PubMed Central PMCID: PMCPMC2677390.
749 13. Sanchez-Pulido L, Pidoux AL, Ponting CP, Allshire RC. Common ancestry of the CENP-A
750 chaperones Scm3 and HJURP. Cell. 2009;137(7):1173-4. doi: 10.1016/j.cell.2009.06.010. PubMed PMID:
751 19563746; PubMed Central PMCID: PMCPMC4397584.
752 14. Dunleavy EM, Roche D, Tagami H, Lacoste N, Ray-Gallet D, Nakamura Y, et al. HJURP is a cell-
753 cycle-dependent maintenance and deposition factor of CENP-A at centromeres. Cell. 2009;137(3):485-
754 97. doi: 10.1016/j.cell.2009.02.040. PubMed PMID: 19410545.
755 15. Pidoux AL, Choi ES, Abbott JK, Liu X, Kagansky A, Castillo AG, et al. Fission yeast Scm3: A CENP-A
756 receptor required for integrity of subkinetochore chromatin. Molecular cell. 2009;33(3):299-311. Epub

757 2009/02/17. doi: 10.1016/j.molcel.2009.01.019. PubMed PMID: 19217404; PubMed Central PMCID:
758 PMCPMC2697330.
759 16. Erhardt S, Mellone BG, Betts CM, Zhang W, Karpen GH, Straight AF. Genome-wide analysis
760 reveals a cell cycle-dependent mechanism controlling centromere propagation. J Cell Biol.
761 2008;183(5):805-18. Epub 2008/12/03. doi: 10.1083/jcb.200806038. PubMed PMID: 19047461; PubMed
762 Central PMCID: PMCPMC2592830.
763 17. Medina-Pritchard B, Lazou V, Zou J, Byron O, Abad MA, Rappsilber J, et al. Structural basis for
764 centromere maintenance by Drosophila CENP-A chaperone CAL1. EMBO J. 2020;39(7):e103234. Epub
765 2020/03/07. doi: 10.15252/embj.2019103234. PubMed PMID: 32134144; PubMed Central PMCID:
766 PMCPMC7110144.
767 18. Schittenhelm RB, Althoff F, Heidmann S, Lehner CF. Detrimental incorporation of excess Cenp-
768 A/Cid and Cenp-C into Drosophila centromeres is prevented by limiting amounts of the bridging factor
769 Cal1. J Cell Sci. 2010;123(Pt 21):3768-79. PubMed PMID: 20940262.
770 19. Orr B, Sunkel CE. Drosophila CENP-C is essential for centromere identity. Chromosoma.
771 2011;120(1):83-96. Epub 2010/09/24. doi: 10.1007/s00412-010-0293-6. PubMed PMID: 20862486.
772 20. Screpanti E, De Antoni A, Alushin GM, Petrovic A, Melis T, Nogales E, et al. Direct binding of
773 Cenp-C to the Mis12 complex joins the inner and outer kinetochore. Curr Biol. 2011;21(5):391-8. doi:
774 10.1016/j.cub.2010.12.039. PubMed PMID: 21353556; PubMed Central PMCID: PMCPMC3074538.
775 21. Petrovic A, Keller J, Liu Y, Overlack K, John J, Dimitrova YN, et al. Structure of the MIS12 Complex
776 and Molecular Basis of Its Interaction with CENP-C at Human Kinetochores. Cell. 2016;167(4):1028-40
777 e15. Epub 2016/11/25. doi: 10.1016/j.cell.2016.10.005. PubMed PMID: 27881301; PubMed Central
778 PMCID: PMCPMC5101189.
779 22. Tanaka K, Chang HL, Kagami A, Watanabe Y. CENP-C functions as a scaffold for effectors with
780 essential kinetochore functions in mitosis and meiosis. Dev Cell. 2009;17(3):334-43. doi:
781 10.1016/j.devcel.2009.08.004. PubMed PMID: 19758558.
782 23. Liu Y, Petrovic A, Rombaut P, Mosalaganti S, Keller J, Raunser S, et al. Insights from the
783 reconstitution of the divergent outer kinetochore of Drosophila melanogaster. Open Biol.
784 2016;6(2):150236. doi: 10.1098/rsob.150236. PubMed PMID: 26911624; PubMed Central PMCID:
785 PMCPMC4772808.
786 24. Przewloka MR, Zhang W, Costa P, Archambault V, D'Avino PP, Lilley KS, et al. Molecular analysis
787 of core kinetochore composition and assembly in Drosophila melanogaster. PloS one. 2007;2(5):e478.
788 doi: 10.1371/journal.pone.0000478. PubMed PMID: 17534428; PubMed Central PMCID:
789 PMCPMC1868777.
790 25. Przewloka MR, Venkei Z, Bolanos-Garcia VM, Debski J, Dadlez M, Glover DM. CENP-C is a
791 structural platform for kinetochore assembly. Curr Biol. 2011;21(5):399-405. PubMed PMID: 21353555.
792 26. Venkei Z, Przewloka MR, Glover DM. Drosophila Mis12 complex acts as a single functional unit
793 essential for anaphase chromosome movement and a robust spindle assembly checkpoint. Genetics.
794 2011;187(1):131-40. PubMed PMID: 20980244.
795 27. Richter MM, Poznanski J, Zdziarska A, Czarnocki-Cieciura M, Lipinszki Z, Dadlez M, et al. Network
796 of protein interactions within the Drosophila inner kinetochore. Open Biol. 2016;6(2):150238. doi:
797 10.1098/rsob.150238. PubMed PMID: 26911623; PubMed Central PMCID: PMCPMC4772809.
798 28. Smoak EM, Stein P, Schultz RM, Lampson MA, Black BE. Long-Term Retention of CENP-A
799 Nucleosomes in Mammalian Oocytes Underpins Transgenerational Inheritance of Centromere Identity.
800 Curr Biol. 2016;26(8):1110-6. doi: 10.1016/j.cub.2016.02.061. PubMed PMID: 27040782; PubMed
801 Central PMCID: PMCPMC4846481.
802 29. Mihajlovic AI, FitzHarris G. Segregating Chromosomes in the Mammalian Oocyte. Curr Biol.
803 2018;28(16):R895-R907. Epub 2018/08/22. doi: 10.1016/j.cub.2018.06.057. PubMed PMID: 30130515.

804 30. Toth A, Jessberger R. Oogenesis: Ageing Oocyte Chromosomes Rely on Amazing Protein Stability.
805 Curr Biol. 2016;26(8):R329-31. Epub 2016/04/27. doi: 10.1016/j.cub.2016.02.059. PubMed PMID:
806 27115691.
807 31. Das A, Black BE, Lampson MA. Maternal inheritance of centromeres through the germline. Curr
808 Top Dev Biol. 2020;140:35-54. Epub 2020/06/28. doi: 10.1016/bs.ctdb.2020.03.004. PubMed PMID:
809 32591081.
810 32. Hemmerich P, Weidtkamp-Peters S, Hoischen C, Schmiedeberg L, Erliandri I, Diekmann S.
811 Dynamics of inner kinetochore assembly and maintenance in living cells. J Cell Biol. 2008;180(6):1101-
812 14. Epub 2008/03/19. doi: 10.1083/jcb.200710052. PubMed PMID: 18347072; PubMed Central PMCID:
813 PMCPMC2290840.
814 33. Jia D, Xu Q, Xie Q, Mio W, Deng WM. Automatic stage identification of Drosophila egg chamber
815 based on DAPI images. Sci Rep. 2016;6:18850. doi: 10.1038/srep18850. PubMed PMID: 26732176;
816 PubMed Central PMCID: PMCPMC4702167.
817 34. Spradling AC. Developmental genetics of oogenesis. In: Bate M, Arias AM, editors. The
818 Development of Drosophila melanogaster. Cold Spring Harbor, NY: Cold Spring Harbor Laboratory Press;
819 1993. p. 1-70.
820 35. Rorth P. Gal4 in the Drosophila female germline. Mech Dev. 1998;78(1-2):113-8.
821 36. Radford SJ, Jang JK, McKim KS. The Chromosomal Passenger Complex is required for Meiotic
822 Acentrosomal Spindle Assembly and Chromosome Bi-orientation. Genetics. 2012;192:417-29. PubMed
823 PMID: 22865736.
824 37. Sugimura I, Lilly MA. Bruno inhibits the expression of mitotic cyclins during the prophase I
825 meiotic arrest of Drosophila oocytes. Dev Cell. 2006;10(1):127-35. PubMed PMID: 16399084.
826 38. Yan D, Neumüller RA, Buckner M, Ayers K, Li H, Hu Y, et al. A regulatory network of Drosophila
827 germline stem cell self-renewal. Dev Cell. 2014;28(4):459-73. Epub 2014/03/01. doi:
828 10.1016/j.devcel.2014.01.020. PubMed PMID: 24576427; PubMed Central PMCID: PMCPMC3998650.
829 39. Baker BS, Hall JC. Meiotic mutants: genetic control of meiotic recombination and chromosome
830 segregation. In: Ashburner M, Novitski E, editors. The Genetics and Biology of Drosophila. 1a. New York:
831 Academic Press; 1976. p. 351-434.
832 40. Hughes SE, Hemenway E, Guo F, Yi K, Yu Z, Hawley RS. The E3 ubiquitin ligase Sina regulates the
833 assembly and disassembly of the synaptonemal complex in Drosophila females. PLoS Genet.
834 2019;15(5):e1008161. Epub 2019/05/21. doi: 10.1371/journal.pgen.1008161. PubMed PMID: 31107865;
835 PubMed Central PMCID: PMCPMC6544331.
836 41. Koehler KE, Boulton CL, Collins HE, French RL, Herman KC, Lacefield SM, et al. Spontaneous X
837 chromosome MI and MII nondisjunction events in Drosophila melanogaster oocytes have different
838 recombinational histories. Nature Genetics. 1996;14:406-14.
839 42. Gyuricza MR, Manheimer KB, Apte V, Krishnan B, Joyce EF, McKee BD, et al. Dynamic and Stable
840 Cohesins Regulate Synaptonemal Complex Assembly and Chromosome Segregation. Curr Biol.
841 2016;26(13):1688-98. Epub 2016/06/14. doi: 10.1016/j.cub.2016.05.006. PubMed PMID: 27291057;
842 PubMed Central PMCID: PMCPMC4942336.
843 43. Tanneti NS, Landy K, Joyce EF, McKim KS. A Pathway for Synapsis Initiation during Zygotene in
844 Drosophila Oocytes. Curr Biol. 2011;21(21):1852-7. PubMed PMID: 22036181.
845 44. Radford SJ, Hoang TL, Głuszek AA, Ohkura H, McKim KS. Lateral and End-On Kinetochore
846 Attachments Are Coordinated to Achieve Bi-orientation in Drosophila Oocytes. PLoS Genet.
847 2015;11(10):e1005605. doi: 10.1371/journal.pgen.1005605. PubMed PMID: 26473960.
848 45. Wang LI, Das A, McKim KS. Sister centromere fusion during meiosis I depends on maintaining
849 cohesins and destabilizing microtubule attachments. PLoS Genet. 2019;15(5):e1008072. Epub
850 2019/06/01. doi: 10.1371/journal.pgen.1008072. PubMed PMID: 31150390; PubMed Central PMCID:
851 PMCPMC6581285.

852 46. Telley IA, Gaspar I, Ephrussi A, Surrey T. Aster migration determines the length scale of nuclear
853 separation in the Drosophila syncytial embryo. J Cell Biol. 2012;197(7):887-95. Epub 2012/06/20. doi:
854 10.1083/jcb.201204019. PubMed PMID: 22711698; PubMed Central PMCID: PMCPMC3384421.
855 47. Unhavaithaya Y, Orr-Weaver TL. Centromere proteins CENP-C and CAL1 functionally interact in
856 meiosis for centromere clustering, pairing, and chromosome segregation. Proc Natl Acad Sci U S A.
857 2013;110(49):19878-83. doi: 10.1073/pnas.1320074110. PubMed PMID: 24248385; PubMed Central
858 PMCID: PMCPMC3856785.
859 48. Dunleavy EM, Beier NL, Gorgescu W, Tang J, Costes SV, Karpen GH. The cell cycle timing of
860 centromeric chromatin assembly in Drosophila meiosis is distinct from mitosis yet requires CAL1 and
861 CENP-C. PLoS Biol. 2012;10(12):e1001460. doi: 10.1371/journal.pbio.1001460. PubMed PMID:
862 23300382; PubMed Central PMCID: PMCPMC3531500.
863 49. Watanabe R, Hara M, Okumura EI, Herve S, Fachinetti D, Ariyoshi M, et al. CDK1-mediated
864 CENP-C phosphorylation modulates CENP-A binding and mitotic kinetochore localization. J Cell Biol.
865 2019;218(12):4042-62. Epub 2019/11/05. doi: 10.1083/jcb.201907006. PubMed PMID: 31676716;
866 PubMed Central PMCID: PMCPMC6891089.
867 50. Stephens AD, Snider CE, Haase J, Haggerty RA, Vasquez PA, Forest MG, et al. Individual
868 pericentromeres display coordinated motion and stretching in the yeast spindle. J Cell Biol.
869 2013;203(3):407-16. Epub 2013/11/06. doi: 10.1083/jcb.201307104. PubMed PMID: 24189271; PubMed
870 Central PMCID: PMCPMC3824013.
871 51. Stephens AD, Haase J, Vicci L, Taylor RM, 2nd, Bloom K. Cohesin, condensin, and the
872 intramolecular centromere loop together generate the mitotic chromatin spring. J Cell Biol.
873 2011;193(7):1167-80. Epub 2011/06/29. doi: 10.1083/jcb.201103138. PubMed PMID: 21708976;
874 PubMed Central PMCID: PMCPMC3216333.
875 52. Hughes SE, Hawley RS. Topoisomerase II is required for the proper separation of
876 heterochromatic regions during Drosophila melanogaster female meiosis. PLoS Genet.
877 2014;10(10):e1004650. doi: 10.1371/journal.pgen.1004650. PubMed PMID: 25340780; PubMed Central
878 PMCID: PMCPMC4207608.
879 53. Heun P, Erhardt S, Blower MD, Weiss S, Skora AD, Karpen GH. Mislocalization of the Drosophila
880 centromere-specific histone CID promotes formation of functional ectopic kinetochores. Dev Cell.
881 2006;10(3):303-15. doi: 10.1016/j.devcel.2006.01.014. PubMed PMID: 16516834; PubMed Central
882 PMCID: PMCPMC3192491.
883 54. Moreno-Moreno O, Torras-Llort M, Azorin F. Proteolysis restricts localization of CID, the
884 centromere-specific histone H3 variant of Drosophila, to centromeres. Nucleic Acids Res.
885 2006;34(21):6247-55. Epub 20061107. doi: 10.1093/nar/gkl902. PubMed PMID: 17090596; PubMed
886 Central PMCID: PMCPMC1693906.
887 55. Dong Q, Yang J, Gao J, Li F. Recent insights into mechanisms preventing ectopic centromere
888 formation. Open Biol. 2021;11(9):210189. Epub 20210908. doi: 10.1098/rsob.210189. PubMed PMID:
889 34493071; PubMed Central PMCID: PMCPMC8424319.
890 56. Nagpal H, Hori T, Furukawa A, Sugase K, Osakabe A, Kurumizaka H, et al. Dynamic changes in
891 CCAN organization through CENP-C during cell-cycle progression. Mol Biol Cell. 2015;26(21):3768-76.
892 Epub 2015/09/12. doi: 10.1091/mbc.E15-07-0531. PubMed PMID: 26354420; PubMed Central PMCID:
893 PMCPMC4626062.
894 57. Hatkevich T, Boudreau V, Rubin T, Maddox PS, Huynh JR, Sekelsky J. Centromeric SMC1
895 promotes centromere clustering and stabilizes meiotic homolog pairing. PLoS Genet.
896 2019;15(10):e1008412. Epub 2019/10/15. doi: 10.1371/journal.pgen.1008412. PubMed PMID:
897 31609962; PubMed Central PMCID: PMCPMC6812850.
898 58. Watanabe Y. Geometry and force behind kinetochore orientation: lessons from meiosis. Nat Rev
899 Mol Cell Biol. 2012;13(6):370-82. doi: 10.1038/nrm3349. PubMed PMID: 22588367.

900 59. Nasmyth K. A meiotic mystery: How sister kinetochores avoid being pulled in opposite directions
901 during the first division. Bioessays. 2015;37(6):657-65. doi: 10.1002/bies.201500006. PubMed PMID:
902 25874377.
903 60. Watanabe R, Hirano Y, Hara M, Hiraoka Y, Fukagawa T. Mobility of kinetochore proteins
904 measured by FRAP analysis in living cells. Chromosome Res. 2022;30(1):43-57. Epub 2022/01/09. doi:
905 10.1007/s10577-021-09678-x. PubMed PMID: 34997387; PubMed Central PMCID: PMCPMC8942963.
906 61. Defachelles L, Raich N, Terracol R, Baudin X, Williams B, Goldberg M, et al. RZZ and Mad1
907 dynamics in Drosophila mitosis. Chromosome Res. 2015;23(2):333-42. Epub 20150314. doi:
908 10.1007/s10577-015-9472-x. PubMed PMID: 25772408; PubMed Central PMCID: PMCPMC4469085.
909 62. Bodor DL, Valente LP, Mata JF, Black BE, Jansen LE. Assembly in G1 phase and long-term stability
910 are unique intrinsic features of CENP-A nucleosomes. Mol Biol Cell. 2013;24(7):923-32. doi:
911 10.1091/mbc.E13-01-0034. PubMed PMID: 23363600; PubMed Central PMCID: PMCPMC3608502.
912 63. Das A, Iwata-Otsubo A, Destouni A, Dawicki-McKenna JM, Boese KG, Black BE, et al. Epigenetic,
913 genetic and maternal effects enable stable centromere inheritance. Nat Cell Biol. 2022;24(5):748-56.
914 Epub 2022/05/10. doi: 10.1038/s41556-022-00897-w. PubMed PMID: 35534577; PubMed Central
915 PMCID: PMCPMC9107508.
916 64. Heeger S, Leismann O, Schittenhelm R, Schraidt O, Heidmann S, Lehner CF. Genetic interactions
917 of separase regulatory subunits reveal the diverged Drosophila Cenp-C homolog. Genes Dev.
918 2005;19(17):2041-53. PubMed PMID: 16140985.
919 65. Głuszek AA, Cullen CF, Li W, Battaglia RA, Radford SJ, Costa MF, et al. The microtubule
920 catastrophe promoter Sentin delays stable kinetochore-microtubule attachment in oocytes. J Cell Biol.
921 2015;211(6):1113-20. doi: 10.1083/jcb.201507006. PubMed PMID: 26668329; PubMed Central PMCID:
922 PMCPMC4687879.
923 66. McKim KS, Joyce EF, Jang JK. Cytological analysis of meiosis in fixed Drosophila ovaries. Methods
924 in molecular biology (Clifton, NJ. 2009;558:197-216. PubMed PMID: 19685326.
925 67. Radford SJ, McKim KS. Techniques for Imaging Prometaphase and Metaphase of Meiosis I in
926 Fixed Drosophila Oocytes. Journal of visualized experiments : JoVE. 2016;116(116):e54666. doi:
927 10.3791/54666. PubMed PMID: 27842371.
928 68. Gilliland WD, Hughes SF, Vietti DR, Hawley RS. Congression of achiasmate chromosomes to the
929 metaphase plate in Drosophila melanogaster oocytes. Dev Biol. 2009;325(1):122-8. doi:
930 10.1016/j.ydbio.2008.10.003. PubMed PMID: 18977343.
931 69. Schittenhelm RB, Chaleckis R, Lehner CF. Intrakinetochore localization and essential functional
932 domains of Drosophila Spc105. EMBO J. 2009;28(16):2374-86. doi: 10.1038/emboj.2009.188. PubMed
933 PMID: 19590494; PubMed Central PMCID: PMCPMC2735171.
934 70. Page SL, Hawley RS. c(3)G encodes a Drosophila synaptonemal complex protein. Genes Dev.
935 2001;15(23):3130-43. PubMed PMID: 11731477.
936 71. Lantz V, Chang JS, Horabin JI, Bopp D, Schedl P. The Drosophila ORB RNA-binding protein is
937 required for the formation of the egg chamber and establishment of polarity. Genes & Dev. 1994;8:598-
938 613.
939

940

941 **Figure 1**

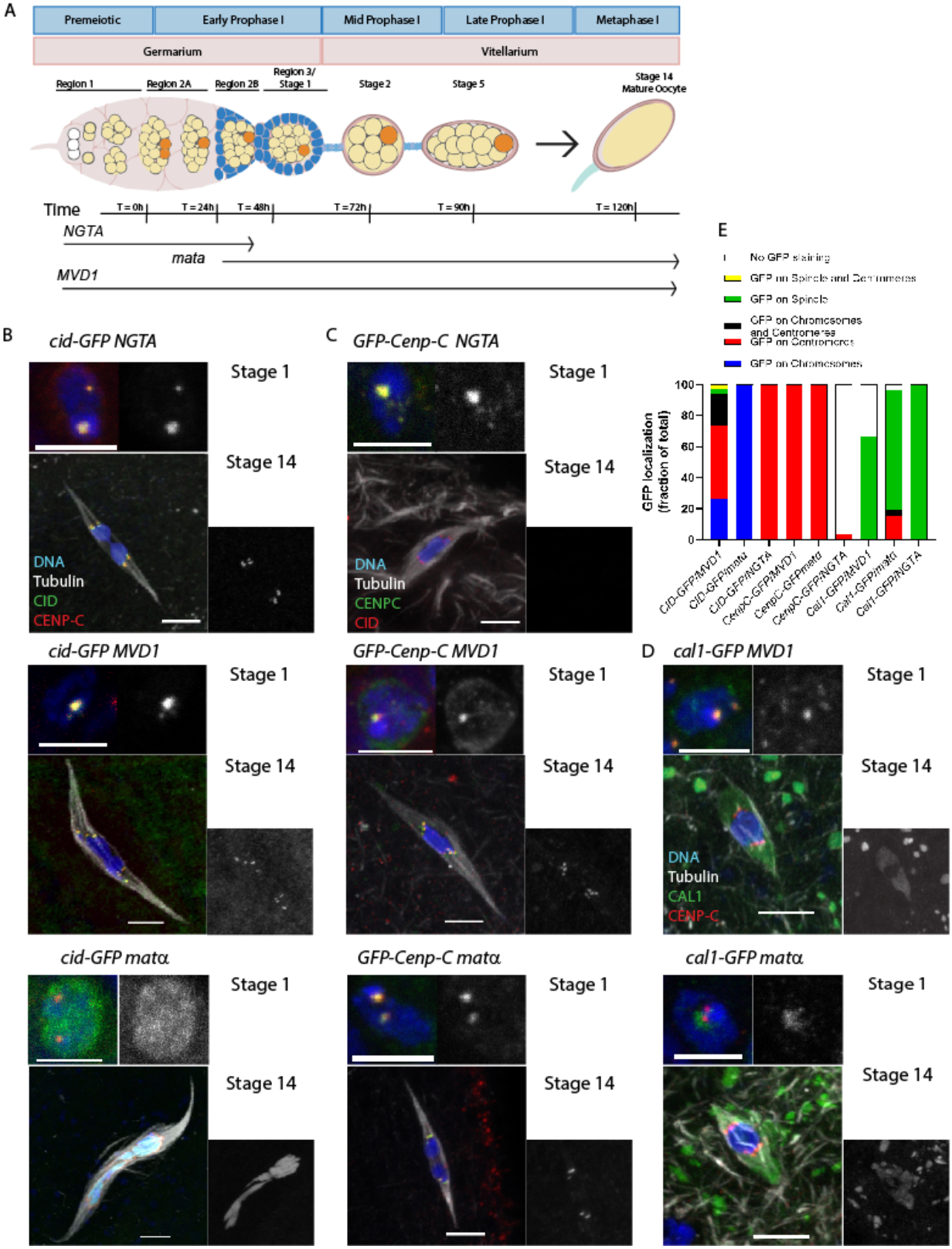

942

943 **Figure 2**

944

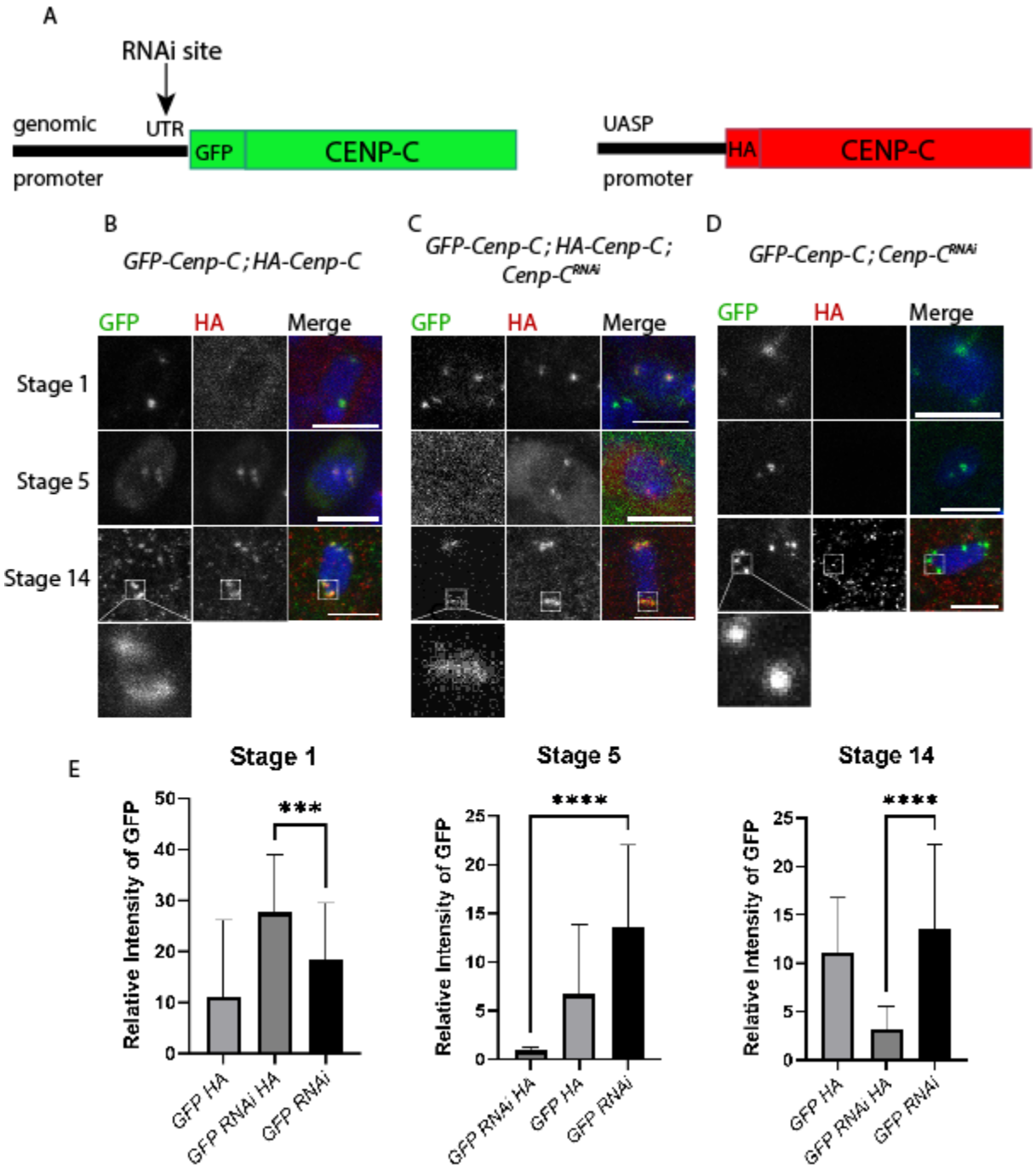

945

946

947 **Figure 3**

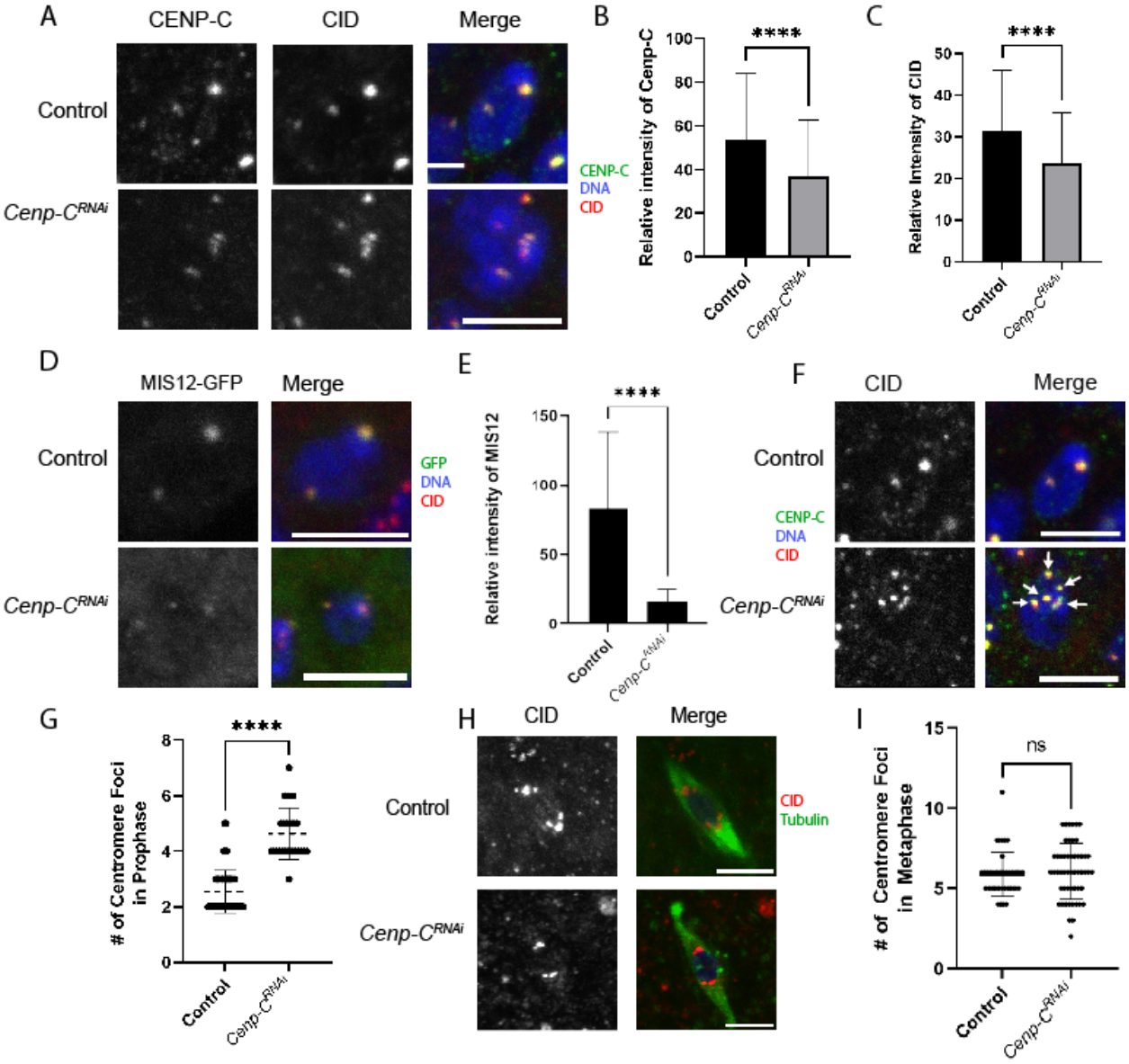

948

949

950

951 **Figure 4**

952

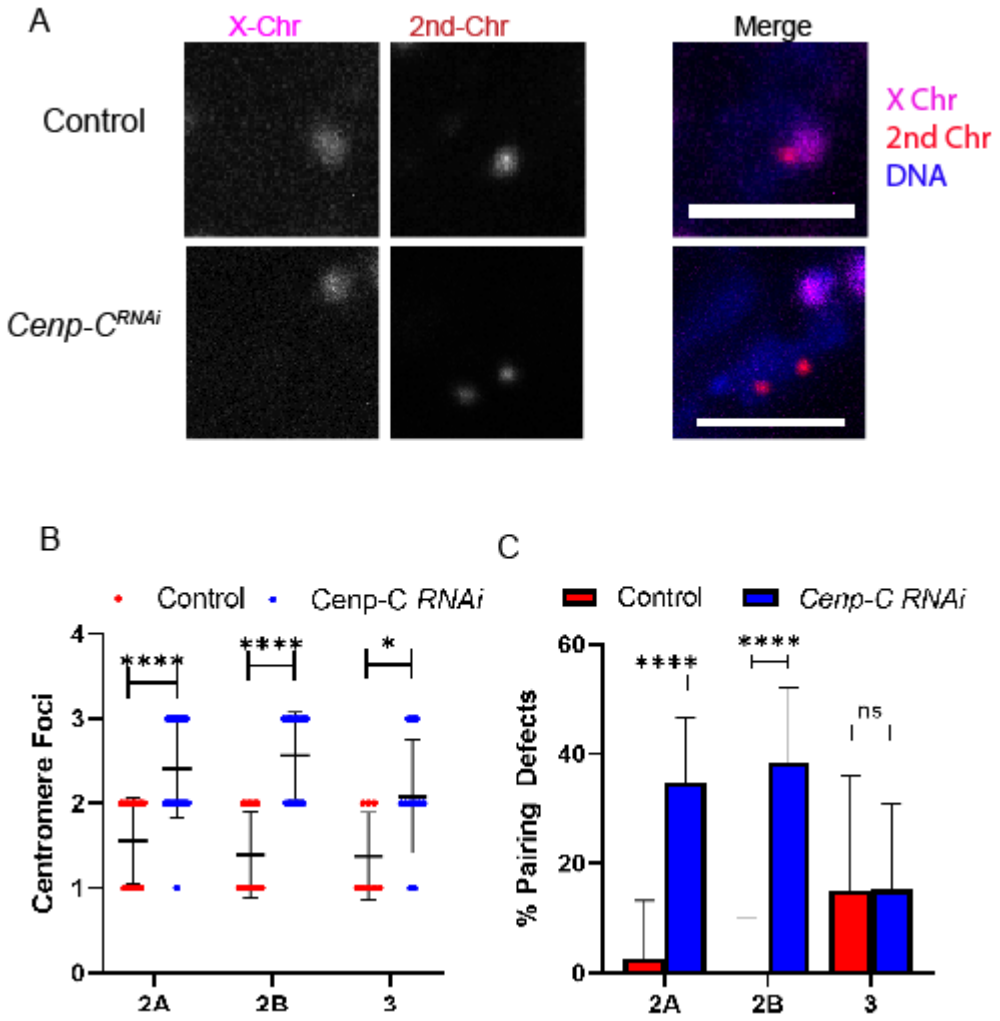

953

954

955

Figure 5

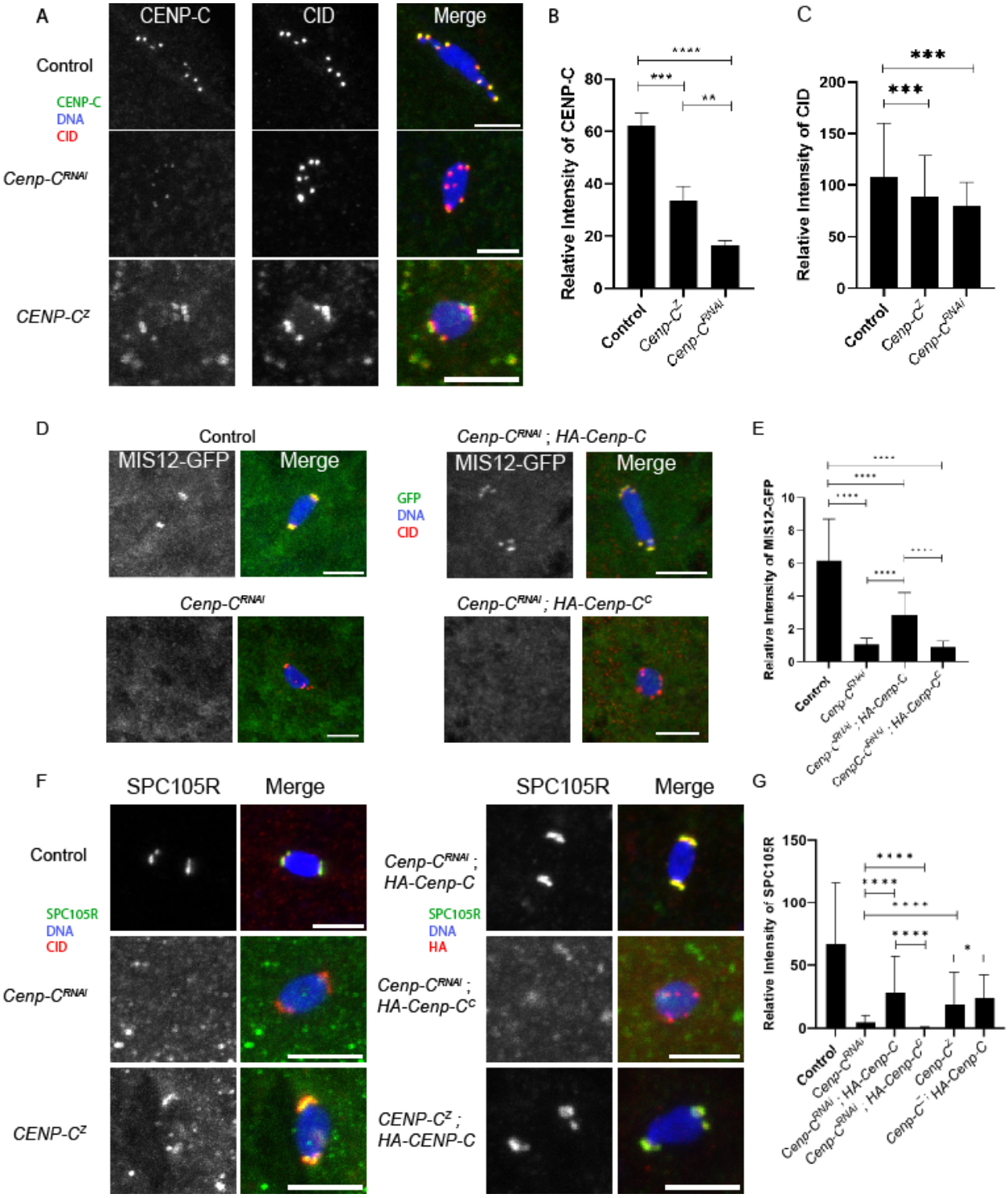
A
CENP-C
CID
Merge
Control
CENP-C
DNA
CID
Cenp-C^RNAi
CENP-C^Z
B
Relative Intensity of CENP-C
Control
Cenp-C^Z
Cenp-C^RNAi
C
Relative Intensity of CID
D
Control
MIS12-GFP
Merge
GFP
DNA
CID
Cenp-C^RNAi ; HA-Cenp-C
Cenp-C^RNAi
Cenp-C^RNAi ; HA-Cenp-C^C
E
Relative Intensity of MIS12-GFP
F
SPC105R
Merge
SPC105R
DNA
CID
HA
Cenp-C^RNAi ; HA-Cenp-C
Cenp-C^RNAi ; HA-Cenp-C^C
CENP-C^Z ; HA-CENP-C
G
Relative Intensity of SPC105R

960 **Figure 6**

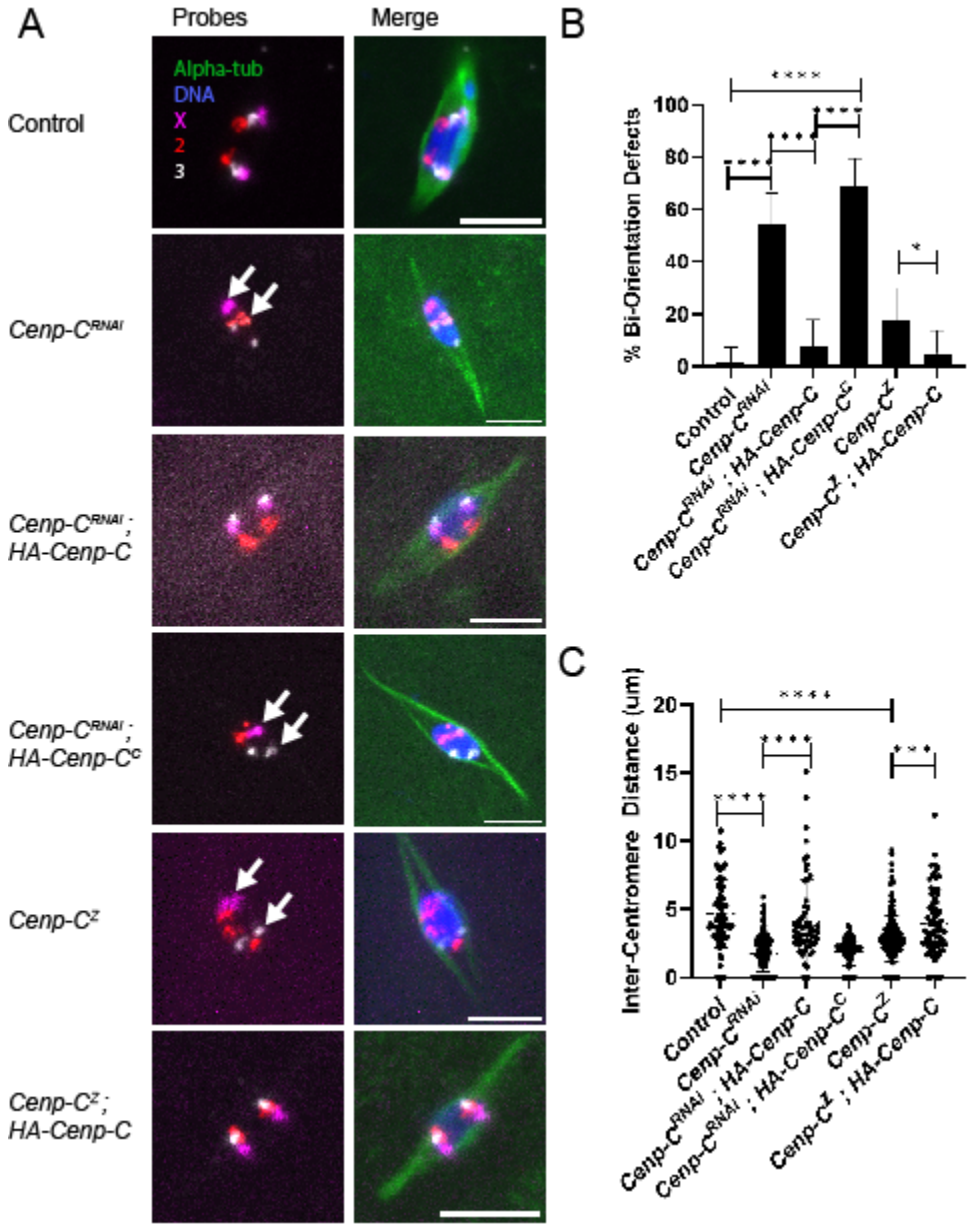

961

962

963

964 **Figure 7**

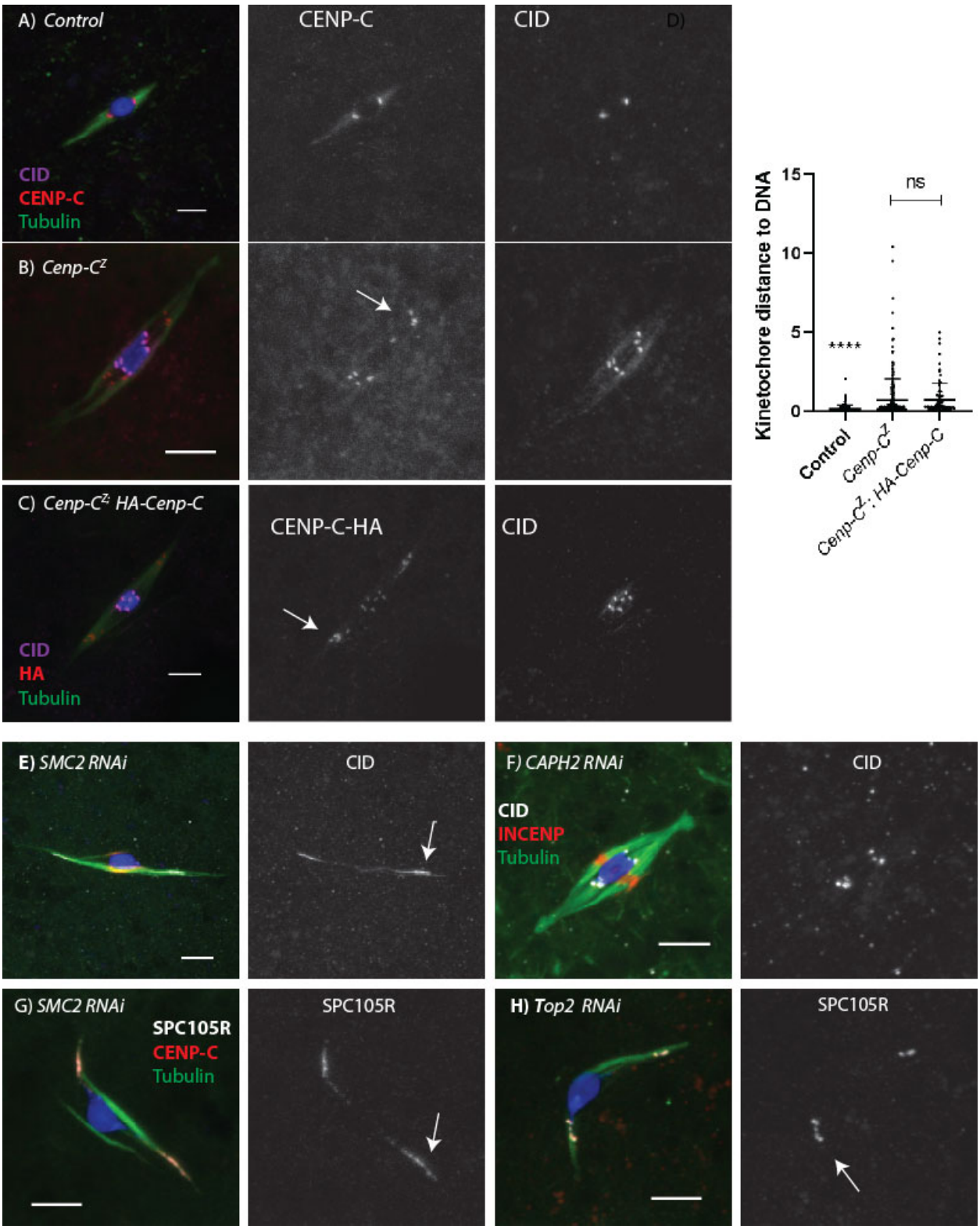

965

966